Title: Variants in USP48 encoding ubiquitin hydrolase are associated with Autosomal Dominant Non-Syndromic Hereditary Hearing Loss
Authors: Sissy Bassani1, Edward van Beelen, Mireille Rossel, Norine Voisin, Anna Morgan, Yoan Arribat, Nicolas Chatron, Jacqueline Chrast, Massimiliano Cocca, Benjamin Delprat, Flavio Faletra, Giuliana Giannuzzi, Nicolas Guex, Roxane Machavoine, Sylvain Pradervand, Jeroen J. Smits, Jiddeke M. van de Kamp, Alban Ziegler, Francesca Amati, Sandrine Marlin, Hannie Kremer, Heiko Locher, Tangui Maurice, Paolo Gasparini, Giorgia Girotto, Alexandre Reymond
Journal: Human Molecular Genetics
Year: 2021
DOI: https://doi.org/10.1093/hmg/ddab145

Variants in USP48 encoding ubiquitin hydrolase are associated with Autosomal Dominant Non-Syndromic Hereditary Hearing Loss

Sissy Bassani[1,2,] Edward van Beelen[3], Mireille Rossel[4], Norine Voisin[1], Anna Morgan[2,5], Yoan Arribat[6], Nicolas Chatron[1,7], Jacqueline Chrast[1], Massimiliano Cocca[5], Benjamin Delprat[4], Flavio Faletra[5], Giuliana Giannuzzi[1,13], Nicolas Guex[9], Roxane Machavoine[10], Sylvain Pradervand[1], Jeroen J. Smits[11], Jiddeke M. van de Kamp[12], Alban Ziegler[10], Francesca Amati[6], Sandrine Marlin[10], Hannie Kremer[11], Heiko Locher[3], Tangui Maurice[4], Paolo Gasparini[2,5], Giorgia Girotto[2,5], Alexandre Reymond[1,*]

[1]Center for Integrative Genomics, University of Lausanne, Lausanne, Switzerland
[2]Department of Medicine, Surgery and Health Sciences, University of Trieste, Trieste, Italy [3]Department of Otorhinolaryngology, Leiden University Medical Center, Leiden, The Netherlands
[4]MMDN, Univ Montpellier, EPHE, INSERM, Montpellier, France
[5]Institute for Maternal and Child Health, IRCCS, Burlo Garofolo, Trieste, Italy
[6]Department of Biomedical Sciences, University of Lausanne, Lausanne, Switzerland
[7]Service de Génétique, Hospices Civils de Lyon, Lyon, France
[9]Bioinformatics Competence Center, University of Lausanne, Lausanne, Switzerland
[10]Centre de référence Surdités Génétiques, Hital Necker, Institut Imagine, Paris, France [11]Department of Otorhinolaryngology and Department of Human Genetics, Donders Institute for Brain, Cognition and Behaviour, Radboud University Medical Center, Nijmegen, The Netherlands
[12]Department of Clinical Genetics, Amsterdam UMC, Vrije Universiteit Amsterdam, Amsterdam, The Netherlands
[13]Present address: Department of Biosciences, University of Milan, 20133 Milan, Italy; Institute of Biomedical Technologies, National Research Council (CNR), 20054 Segrate, Italy [*]Correspondence should be addressed to: Alexandre Reymond, Center for Integrative Genomics, Genopode building, University of Lausanne, CH-1015 Lausanne, Switzerland, phone: +41 21 692 3930, fax; +41 21 692 3965, email: alexandre.reymond@unil.ch

Abstract

Non-Syndromic Hereditary Hearing Loss (NSHHL) is a genetically heterogeneous sensory disorder with about 120 genes already associated. Through exome sequencing and data aggregation, we identified a family with six affected individuals and one unrelated NSHHL patient with predicted-to.be deleterious missense variants in USP48. We also uncovered an eighth patient presenting unilateral cochlear nerve aplasia and a de novo splice variant in the same gene. USP48 encodes a ubiquitin carboxyl-terminal hydrolase under evolutionary constraint. Pathogenicity of the variants is supported by in vitro assays that showed that the mutated proteins are unable to hydrolyze tetra-ubiquitin. Correspondingly, three-dimensional representation of the protein containing the familial missense variant affects a loop that controls binding to ubiquitin. Consistent with a contribution of USP48 to auditory function, immunohistology showed that the encoded protein is expressed in the developing human inner ear, specifically in the spiral ganglion neurons, outer sulcus, interdental cells of the spiral limbus, stria vascularis, Reissner's membrane, and in the transient Kolliker's organ that is essential for auditory development. Engineered zebrafish knocked-down for usp48, the USP48 ortholog, presented with a delayed development of primary motor neurons, less developed statoacoustic neurons innervating the ears, decreased swimming velocity and circling swimming behavior indicative of vestibular dysfunction and hearing impairment. Corroboratingly, acoustic startle response assays revealed a significant decrease of auditory response of zebrafish lacking usp48 at 600Hz and 800Hz wavelengths In conclusion, we describe a novel autosomal dominant NSHHL gene through a multipronged approach combining exome sequencing, animal modeling, immunohistology and molecular assays.

Introduction

Hearing loss is the most common sensory disorder affecting an estimated 6% of the population (WHO -https://www.who.int/health-topics/hearing-loss#tab=tab_1). Approximately 60% of the cases of inherited deafness are due to malfunction of inner ear structures such as the cochlea and the auditory nerve(1). Its hereditary fraction can be divided in syndromic, (.30% of cases) and non-syndromic (.70% of cases) forms. Notwithstanding that approximately 120 genes have already been associated with Non-Syndromic Hereditary Hearing Loss (NSHHL)(2), the current genetic tests fail to provide a diagnosis in almost half of the cases(3). This suggests that many novel deafness genes still need to be characterized.

Zebrafish are becoming a popular model for hearing loss studies due to their rapidly development of morphological specializations for hearing. From five days post fertilization (dpf), they detect sound waves(4), allowing researchers to test their auditory capacity through acoustic startle response(5). From a genetic point of view, more than 50 genes are known to impact the auditory inner ear and the vestibular system of zebrafish(5), and many of these genes are conserved and associated with the inner ear development and function in other vertebrates, including humans(6, 7). These features combined with their rapid development, ease of maintenance and accessibility to the inner ear, make zebrafish an attractive and suitable model to investigate the development and molecular genetics of the vertebrate inner ear.

Members of the ubiquitin-specific proteases family have been associated with hearing loss. Specifically, the catalytically inactive tight junction-associated Usp53 was shown to be essential for the survival of auditory hair cells and normal hearing in mice(8), while variants in the dog USP31 were associated with adult-onset deafness in border collies(9). Histological findings further support the involvement of ubiquitin in hearing as ubiquitin-positive granules were identified in the neuropil of cochlear nuclei of aging dogs(10). In this study we combined exome sequencing (ES), data aggregation from multiple laboratories, animal modeling and molecular assays to associate USP48 (MIM: 617445) variants with an autosomal dominant NSHHL (ADNSHHL). Intriguingly, both USP31 and USP48 regulate the nuclear factor-.B(11), whose deficiency was associated with auditory nerve degeneration and increased noise-induced hearing loss(12).

Results

Within our NSHHL Italian families, we analyzed a four-generation family with six affected individuals (Figure 1A; Supplementary Figure S1). The proband (IV:2) presented with slight (low frequency) to severe (mid-to high-frequencies) bilateral sensorineural hearing loss and was first diagnosed at 8 years of age and is using hearing aids since.. Tympanometry revealed a tympanogram type A. While otoacoustic emissions have not been tested, clinical evaluation showed no motor or vestibular problems. CT, MRI, an ophthalmological evaluation and a thyroid and dysmorphological assessments resulted normal. Her mother (III:2) presented moderate (mid-frequencies) to slight (high frequencies) bilateral sensorineural hearing loss, whereas her maternal uncle (III:1) showed severe (low frequencies) to profound (mid- to high-frequencies) bilateral sensorineural hearing loss. Hearing loss requiring prosthesis was diagnosed in the maternal grandmother (II:2) at 50 years of age. She showed moderate (low frequencies) to severe (mid-frequencies) to profound (high frequencies) bilateral sensorineural hearing loss. Her brother (II:3) is affected by severe hearing loss across all frequencies with his left ear reaching a moderate

loss at the 4 kHz. His deafness was recognized at birth and worsened in adulthood (Figure 1A; Supplementary Figure S1).

As targeted screening of the commonest 99 deafness genes in the affected subjects was negative, the affected individuals IV:2, III:1, III:2 and II:3, as well as the unaffected members IV:1 and III:3 of the family (Figure 1A-B) were subjected to ES. These analyses showed that no rare variant segregated with the disease made exception of a missense variant in USP48 NC_000001.10:g.22056281C>T, NM_032234.7:c.1216G>A, NP_115612.4:p.(Gly406Arg) (GRCh37/hg19) (Figure 1A-B). While it is predicted to be deleterious by multiple prediction tools (PolyPhen-2: possibly damaging, score = 1; SIFT: deleterious, CADD = 29.1, GERP = 5.44), this variant is present in GnomAD v2.1.1 with a minor allele frequency (MAF) of 6.7x10-5 (17 allele out of 251,304 with no homozygotes). Consistent with the presence of this variant in supposedly healthy individuals, we observed an incomplete penetrance of the disease within our family, with one hearing individual (III:4) heterozygote for this variant Figure 1A-B. His most recent audiometric evaluation was performed in 2019 at 39 years of age (Supplementary Figure S1). This is consistent with the notion that many of the developmental disorder genes awaiting discovery are likely to be less penetrant than the currently known genes(13). Note also that while GnomAD "has made every effort to exclude individuals with severe pediatric diseases, they do not rule out the possibility that some of their participants do actually suffer from a disease of interest". No other rare variant segregated with the disease.

USP48 is expressed in the human cerebellum and cerebellar hemisphere (The Human Protein ATLAS; Genome Browser) and in the cochlear and vestibular sensory hair cells of mice and zebrafish (gEAR Portal 2020). It is often somatically mutated in the pituitary adenomas, i.e. Cushing's disease (14, 15). This gene is under evolutionary constraint with five observed loss of function variants (LoF, i.e. truncation variant) versus 65 expected (ratio o/e = 0.08 [0.04-0.16]; pLI (probability of LoF intolerance) = 1) and 256 observed missense variants versus 548 expected (o/e = 0.47 [0.42-0.52]; Z = 4.37) in GnomAD. Whereas intolerance to truncating variants is customarily used to narrow down lists of causative variants in autosomal dominant intellectual disability and syndromic developmental disease we wondered if this was a good selection criterion when searching for genes associated with autosomal dominant NSHHL (ADNSHHL). To evaluate this criterion, we assessed the distribution of o/e LoF ratio of the 46 known ADNSHHL genes (Supplementary Table S1). While some ADNSHHL genes are not constrained especially the prevalent ones (e.g., GJB2 o/e = 2.62 and GJB6 o/e = 1.07), we observed that 30 out of 46 ADNSHHL genes (65%) present with an o/e LoF ratio below 0.5. This result suggests that the majority of dominant non-syndromic deafness genes are under evolutionary pressure (o/e median = 0.37; Figure 2C) and that this can be used as a selection criterion upon screening for novel rare ADNSHHL causative genes. Of note, USP48 belongs to the list of genes enriched in 'brain-critical exons', that are often prioritized in genotype-phenotype studies of neurodevelopmental conditions(16).

Our search for more cases led to the identification of one Dutch NSHHL affected individual who presented with progressive hearing loss starting at 24 years of age without additional syndromic features. At 40 years of age his audiogram, displayed moderate to severe sensorineural hearing loss at all frequencies with asymmetry between both ears. A computed tomography of the bilateral temporal bones did not show abnormalities.

ES of this patient identified a predicted-to-be deleterious missense variant in USP48 NC_000001.10:g.22032676_22032677delinsAA, NM_032236.7:c.2215_2216delinsTT, NP_115612.4:p.(Thr739Leu) (CADD=23.3; GnomAD MAF=6.3x10-5). His mother complained of hearing loss since the age of 27 years that progressed to profound hearing loss. A maternal uncle was similarly reported to be hearing impaired. Whereas such a pedigree suggests autosomal dominant inheritance of hearing impairment, as the mother and maternal uncle did not consent samples, we were not able to confirm transmission (Figure 1A). We uncovered an eighth affected individual in France presenting with right profound sensorineural hearing impairment diagnosed at 12 months, while left hearing was still normal during the last clinical genetic consultation (at 6 years old). Suggestive of a right cochlear nerve aplasia or hypoplasia, MRI of cerebral and internal auditory canals could not visualize the right cochlear nerve. Temporal bone CT scan was normal. This patient is heterozygote for a de novo splice variant in USP48 (NC_000001.10:g.22013682A>G, NM_032236.7:c.3058+2T>C, NP_115612.4:p.?; GnomAD MAF=0)(Figure 1A). This variant abolishes the donor site according to MaxEntScan, NNSplice and SpliceAI (score=0.97). This would result in a frameshift meaning that either the encoded RNA would be recognized by NMD and degraded, or it will encode a truncated protein, which we showed has lost its enzymatic activity (Figure 2D). These splice predictors also suggest that the next GT will not be used because of a unfavorable preceding TTT stretch, which should result in the addition of ten new residues before a TGA opal stop codon p.(Val1020Glyext*9). Would this be the case or alternatively if the intron is retained, we hypothesize that the corresponding RNA will undergo non.sense mediated decay. While we cannot exclude that the association between the French patient and USP48 is spurious before identification of other similarly affected individuals, we think that it is important to document this case.

USP48 encodes a ubiquitin carboxyl-terminal hydrolase able to recognize and hydrolyze the Glycine or Lysine peptide bond at the carboxy-terminus of ubiquitin. While the amino-terminus of USP48 contains the ubiquitin carboxyl-terminal hydrolase domain (residues 86-457), its C-terminal part comprises three sequential DUSP (domain present in ubiquitin-specific proteases) from residues 465 to 548, 571 to 686 and 714 to 1004. DUSPs are present in other ubiquitin-specific proteases, such as USP4, USP11 and USP15 and help them determine their biological activity and specificity of binding(17). For example, the DUSP-Ubl domain of USP4 was shown to be necessary to enhance ubiquitin dissociation and achieve full catalytic turnover(18). The pathogenicity of the Italian variant is supported by the three-dimensional representation of the encoded peptide. The mutated residue is located within a flexible loop that flanks over the catalytic site of the hydrolase and could play a role in substrate specificity (Figure 2A). Of note the Met415 residue, often found somatically mutated in Cushing's disease, i.e. adenomas of the pituitary(14, 15), is only a few residues after the end of the loop bearing Gly406, in a stretch of residues [AYMLVY] conserved in USP48 orthologs and in a region positioned close to ubiquitin (< 8 Å) and within 12 Å of active site residues Cys98 and His353 (Figure 2A). The Thr739, residue mutated in the Dutch patient, is situated in a conserved T-D-[VE].L-Y stretch found in 185 Swiss-Prot sequences. A search for templates using HHPRED(19) identified a DUSP (domain present in USPs) fold (pdb entry 3LMN; DOI 10.2210/pdb3LMN/pdb). NetPhos 3.1(20) predicts that Thr739 could be phosphorylated by CKII or an unspecified kinase (score of 0.508 and 0.755, respectively), whereas Src could be phosphorylating the neighboring Tyr743 (0.505). These kinases have been identified in a screen for enzymes involved in ototoxic damage to the murine organ of Corti(21).

Mutation of this threonine residue could affect phosphorylation status and protein-protein interaction as it is exposed on the surface of the DUSP domain (Figure 2B).

We then assessed in vitro the effect of the USP48 variants on the activity of the encoded ubiquitin carboxyl-terminal hydrolase. The peptides FLAG-USP48WT (wild-type), FLAG-USP48C98S, encoding a catalytically dead enzyme, FLAG-USP48G406R, FLAG-USP48T739L and FLAG-USP481.1019 that encodes only the first 1019 amino-terminal residues of the protein and mimics the French variant, were expressed in HEK293T cells. We assessed the ability of the corresponding anti-FLAG immunoprecipitated extracts to hydrolyze ubiquitin upon incubation with tetra-ubiquitin. We observed that like the catalytically dead enzyme and contrary to the wild-type molecule, the truncated USP48 hydrolase and the ones containing the ADNSHHL missense variants identified in the Italian and Dutch affected individuals showed an impaired ability to cleave tetra-ubiquitin into tri-, di- and mono-ubiquitin (Figure 2D).

Consistent with a contribution of USP48 to auditory function and according to the gEAR portal, the orthologous transcript is found in different types of cells of P1 mouse cochlear epithelium. Using immunohistology, we then showed that the human USP48 protein is present in fetal inner ear specimens. In inners ears of W12 and W14 old human fetuses, we found antigens recognized by anti.USP48 antibodies in the cytoplasm of supporting cells within the Kolliker's organ, the earliest epithelial structure present in the developing auditory sensory organ(22), in interdental cells, in cells of the outer sulcus, in the Reissner's membrane and in fibrocytes of the spiral ligament (Figure 3A). Transient expression was observed in intermediate cells of the stria vascularis at W14 (Figure 3A), but not at W12 (Figure S2A). Spiral ganglion neurons and the surrounding mesenchyme also expressed USP48 (Figure 3B). In addition, USP48 is present in the vestibular system, in particular in supporting cells of the saccular macula and ampulla, the periotic mesenchyme, the neuronal cell bodies of the Scarpa's ganglion and the epithelial cells of the semicircular canals of W15 embryos (Figure 3C, Figure S2B-C). No expression was seen in the inner or outer hair cells of the cochlea and in the hair cells of the vestibular system at these developmental stages.

To gain insight into the function of USP48, we ablated the orthologous usp48 in zebrafish by CRISPR/Cas9 genome editing(23). While a knock-in of one the missense variant would have more accurately modelled the affected individuals, the engineered knock-down still mimics the decrease in ubiquitin carboxyl-terminal hydrolase enzymatic activity observed in our in vitro assays and the truncation variant. We engineered F0 larvae using three different small guide RNAs targeting exons 4 (gusp48-4), 9 and 10 of usp48 and assessed their locomotion and touch response. Swimming in circle upon touching was suggested to be an indicator of vestibular dysfunction and auditory impairment(24). At 3 dpf we observed that an increased fraction of crispant animals swam in circle in response to a tactile stimulus compared to wild-type and mock-treated fish (Figure 4A). Similarly, 5 dpf mutant larval batches showed a reduction in both global velocity and net speed (Figure S4). The gusp48 targeting exon 4 appeared as the most efficient guide with notable effects on global velocity (gusp48-4+Cas9 (treated) 1.0 versus gusp48-4 (mock-treated controls) 1.4 mm/s; $p = 0.04$), net speed (5.4 versus 6.1 mm/s; $p = 0.01$) and tactile response assays (78% versus 12% miss-responding) (Figure 4A, Figure S4). We assessed the presence of microdeletion and showed that gusp48-4 induced genetic editing in 75% of injected embryos (founders, F0). We then tested the auditory startled responses of usp48 mutant larvae at 5 dpf. Consistent with hearing impairment they presented with a significantly decreased

response to white noise ($p = 0.05$; Figure 4B). Upon stratifying by frequency, we found that usp48 knocked-down fish larvae presented with a significantly decreased reaction when compared to wild-type and mock treated fish towards 600 Hz ($p = 0.03$) and 800 Hz ($p = 0.0017$) pulses but not to the shorter 400 Hz ($p = 0.18$) and longer 1000 Hz ($p = 0.16$) frequencies (Figure 4B). This impaired response to acoustic cues was not complemented by changes in the response to light as we observed no differences in the visual motor response of usp48 knocked-down, wild-type and mock treated fish larvae during light-dark transitions (Figure S5). To possibly uncover the origin of this hearing impairment, we first analyzed the development of sensory hair cells of usp48 knocked-down zebrafish. We investigated both AB-line zebrafish dyed with YO-PRO-1 that selectively labels neuromast hair cells and Brn3c:mGFP/NBT:dsRED zebrafish whose hair cells of the inner ear and lateral line neuromasts are labeled green while neurons are stained in red. The superficial sensory hair cells of usp48 knocked-down fish showed a normal mechano-transduction function and the neuromasts presented a regular superficial distribution along the anterior (head) and posterior (trunk and tail) lateral-line systems (Figure S6). We then assessed the development of the neuronal system and discovered that the vestibulo-acoustic neurons innervating the ear bases were less developed in 5 dpf usp48 knocked-down than in mock-treated and wild-type fish. These fish presented with less organized and significantly less statoacoustic neurons when compared with mock-treated fish (36.0 ± 6.4 versus 52.3 ± 8 neurons, $p = 0.01$) and wild-type fish (51.5 ± 2.1, $p = 0.02$) (Figure 4C-D). In addition, usp48 crispants showed a significant delay in the development of primary motor neurons at 28 hpf that got exacerbated at 48 hpf (Figure S7). During early development the size of 1 dpf usp48 knocked-down embryos was smaller when compared to that of mock-treated and wild-type animals ($p = 0.02$) (Figure S8). The subsequent development of the swim-bladder, a double-chambered organ located in the coelom used to maintain buoyancy that may also function as an acoustic resonator appeared slower in treated fish (data not shown) suggesting a general delay in the development of usp48 knock-downs.

Discussion

We describe three families with ADNSHHL. The affected individuals of the first two families presented with bilateral hearing loss and heterozygosity of predicted-to-be deleterious missense variants in the ubiquitin carboxyl-terminal hydrolase USP48, while the affected individual of the third family exhibited unilateral cochlear aplasia-associated hearing loss and a de novo splicing variant in the same gene. Whereas further cases are warranted to demonstrate if a single or multiple pathological processes are associated with missense and truncation variants, we showed that the Italian, Dutch and French variants impair the enzymatic activity of the encoded enzyme and that zebrafish ablated for the orthologous usp48 are hearing impaired. Together these data and the observation that there is a significant paucity of USP48 truncation variants in the human population suggest haploinsufficiency as mechanism of action. Of note the phenotypic variability amongst the affected individuals of the Italian family cannot be explained by the presence of more than one genetic cause of hearing loss as the targeted screening of variants in the commonest 99 deafness genes was negative. We observed expression of USP48 in the human fetal spiral ganglion and Scarpa's neurons, as well as a general developmental delay of the neuronal system of usp48 knocked-down zebrafish. These crispants presented with significantly less statoacoustic neurons and a decreased acoustic startle response suggesting that the USP48-

encoded ubiquitin carboxyl-terminal hydrolase is important to auditory function. USP48 also controls the E3 ubiquitin-protein ligase Mdm2(25) (MIM: 164785), which ubiquitinates and antagonizes p53 (MIM: 191170). USP48 role in controlling DNA repair is further highlighted by its function as a histone H2A deubiquitinase that counteracts BRCA1 E3 ubiquitin-ligase activity(26) (breast cancer 1; MIM: 113705) and by the reduced chromosomal instability of Fanconi anemia cells upon knock-down of USP48(27, 28). USP48 was also shown to regulate the stability of TRAF2 (tumor necrosis factor receptor-associated factor 2; MIM: 601895) thus controlling E-cadherin-mediated adherens junctions. Such junctions are important for cochlear development and growth of auditory neurons(29). The expression level of E-cadherin is determinant for hair cell differentiation; its level inversely correlates to the capacity of supporting cells to differentiate into sensory hair cells(30). Data suggest that in the absence of sound, developing cochlear and primary auditory neurons undergo experience-independent activity. Two hypotheses were suggested for this activity: the inner supporting cells of the Kolliker's organ, an organ only present during the critical period of auditory development, release ATP hence recapitulating auditory neuron activity or alternatively inner hair cells (IHCs) generate this spontaneous activity without ATP activation(22, 31). Nevertheless, it was proposed that "developmental abnormalities of the Kliker's organ may lead to congenital hearing loss as mutations in ion channels important for its activity (e.g. GJB2, GJB6) are associated with deafness"(22). Whereas E-cadherin is present in outer hair cells, it is not expressed in IHCs or in the part of the Kolliker's organ in contact with them. We similarly observe expression of USP48 in the Kolliker's organ, but not in the developing IHCs.

In conclusion we have identified a new ADNSHHL candidate gene. Our results support adding USP48 to the list of genes associated with hearing function and to future HHL diagnostic panels. Our findings also emphasize the importance of the temporary Kolliker's organ in auditory development.

Materials and Methods

Ethical Approval

Each participant signed consent forms for clinical studies. In Italy, the research approval was obtained from the Institutional Review Board of IRCCS Burlo Garofolo, Trieste. The study of the Dutch subject was approved by the medical ethics committee of the Radboudumc (registration number: NL33648.091.10). The research was conducted according to the ethical standards defined by the Helsinki Declaration. Use of human fetal specimens was in accordance with the Dutch legislation (Fetal Tissue Act, 2001) and the WMA Declaration of Helsinki guidelines. Approval was obtained from the Medical Research Ethics Committee of Leiden University Medical Center (protocol registration number B18.044). Written informed consent of the donors was obtained following the Guidelines on the Provision of Fetal Tissue set by the Dutch Ministry of Health, Welfare and Sport (revised version, 2018).

Clinical description

The hearing loss is defined by World Health Organization (WHO) as a speech-frequency pure tone average > 25 dB at 500, 1000, 2000, and 4000 Hz in the better hearing ear(32). In particular, disabling deafness is described as loss of auditory ability > 40 dB in adults and > 30 dB in children, in the better hearing ear" (see who.int/news-room/fact-sheets/detail/deafness-and-hearing-loss). Deafness can be classified in different degrees from mild (26 dB -40 dB), moderate (41 dB -

55 dB), moderately severe (56 dB - 70 dB), severe (71 dB - 90 dB) up to profound hearing loss (≥ 91 dB)(33).

All NSHHL living affected individuals of the Italian family underwent a clinical ENT examination. Hearing function was assessed by pure-tone audiometry, tympanogram, and oto-acoustic emissions (Supplementary Figure S1). Other clinical tests were carried out to exclude syndromic forms. The French proband is the second child of unrelated parents of French origin without any familial medical history (Guyana and French metropolis). She was born at term (38+3 GW) from a dizygotic twin pregnancy with normal weight (2830 g), length (46 cm) and head circumference (33cm). She had good psychomotor development, sitting at six months, walking at 16 months.

Genetic Analyses

Italian family: DNA was extracted from peripheral blood using a QIAsymphony instrument (Qiagen) and quantified with a Nanodrop ND-1000 spectrophotometer (NanoDrop Technologies). The family was sequentially assessed for causative variants in GJB2 (MIM: 121011), GJB6 (MIM: 604418), MTRNR1 (MIM: 561000) and a panel of 96 deafness genes by targeted resequencing(34) with negative results. Exome sequencing was performed using the Ion ProtonTM platform according to the manufacturer's protocols (Life Technologies). Briefly, 1 .g of genomic DNA was used to construct DNA libraries using the Ion AmpliSeqTM Exome Kit. The overall mean-depth base coverage was 102-fold, while on average 89% of the targeted region was covered at least 20-fold.

Read mapping and variant calling were performed using Ion TorrentSuite v4.0 software (Life-Technologies). Variants were filtered using Varapp according to quality of the calling, their frequency in control populations (. 1% in 1000genome and Genome Aggregation Database (GnomAD) v2.1.1) and their predictive impact on the function of the protein (high and medium impact in PolyPhen-2 and SIFT databases, GERP score . 3.00 and CADD (scaled) . 10.00) as described(35) and an autosomal dominant inheritance scenario. Sanger sequencing was used to confirm segregation.

Dutch proband: Exome capture, sequencing and variant filtering was performed as previously described in particular no likely pathogenic variant was identified in a list of 156 known deafness genes(36).

French proband: DNA was extracted from leucocytes from the proband and her parents. An array-CGH (400kb resolution) was normal. Exome capture was performed with the Sure Select Human All Exon kit (Agilent Technologies). Agilent Sure Select Human All Exon (58 Mb, V6) libraries were prepared from 3 .g of genomic DNA sheared with an Ultrasonicator (Covaris) as recommended by the manufacturer. Barcoded exome libraries were pooled and sequenced with a HiSeq2500 system (Illumina), generating paired-end reads. After demultiplexing, sequences were mapped on the human genome reference (NCBI build 37, hg19 version) with BWA. Variant calling was carried out with the Genome Analysis Toolkit (GATK), SAMtools, and Picard tools. Single-nucleotide variants were called with GATK Unified Genotyper, whereas indel calls were made with the GATK IndelGenotyper_v2. All variants with a read coverage ≤2. and a Phred-scaled quality ≤20 were filtered out. The overall mean-depth base coverage of the trio was between 142 and 217-fold, while more than 99% of the targeted region was covered at least 15-fold. Variant-filtering strategies especially familial segregation led to the identification of only one candidate variant: a de novo affecting a splice donor site in USP48.

Ubiquitin hydrolase activity assay

The plasmids pcDNA3 expressing hUSP48 wild-type (FLAG-USP48WT; ENST00000308271.14) and a catalytically dead enzyme (FLAG-USP48C98S) were donated by Dr. G. Mosialos, Aristotle University of Thessaloniki(37). The USP48 mutations identified in the Italian, French and Dutch probands were engineered using the QuikChange II XL Site-Directed Mutagenesis Kit (Agilent Technologies) following the manufacturer's instructions. The FLAG-USP481-1019 encoding a truncated protein was engineered by site-directed mutagenesis of the Gln1019 CAA codon into an ochre TAA stop codon. Sanger sequencing confirmed each variant. HEK293T cells were transfected with FuGene (FuGene Hd Transfection, #E2312, Promega). Cells were cultured at 37°C under 2 to 4% CO2 in DMEM supplemented with 10% FBS and 1% Pen/Strep. Cells were lysed 24 or 48 hours after the transient transfection in RIPA buffer (#20-188, Millipore) supplemented with proteases inhibitors (Halt Protease & Phosphatase inhibitor cocktail, #78440, Thermo Scientific). The protein lysate concentration was determined by BCA Assay (Pierce, BCA Protein Assay Kit #23227, Thermo Scientific). Equal amounts of proteins were resolved on 4-15% SDS-PAGE mini-gels and transferred to nitrocellulose membranes (GE Healthcare, Life Science) to assess FLAG-USP48 expression. Immunoblots were blocked in 5% milk powder in TBST (50 mM Tris-HCl, pH 7.4, 200 mM NaCl, and 0,1% Tween 20) for 1h at room temperature (RT). Membranes were incubated overnight at +4°C with primary antibodies: anti-Flag 1:20000 (#F3165, anti-Mouse, Sigma) and anti-.-actin 1:2500 (anti-Rabbit, Sigma) diluted in TBST. Secondary antibodies: anti-Mouse-HRP (#W402B, Promega) and anti-Rabbit-HRP (#sc-2030, Santa Cruz Biotechnology) were diluted, 1:2500 and 1:5000 respectively, in TBST and incubated for 1h at RT. Reactive bands were detected with ECL detection kit (Immobilon Western Kit, Millipore). Ubiquitin hydrolase activity assay were performed as described(37). Briefly, wild-type or mutated FLAG-tagged USP48 proteins were immunoprecipitated from cell lysates without protease inhibitors 48h post-transfection. Immunoprecipitated proteins were incubated with 0.8/1 ug of tetraubiquitin molecules (63-linked polyubiquitin chain, Boston Biochem). Reactions were separated by SDS-PAGE followed by Coomassie staining.

Protein model

A USP7 (MIM: 602519) model was built using Swiss-PdbViewer (spdbv)(38) as described(39)(39). The chain C of pdb entry 4YOC(40) was superposed onto pdb entry 5J7T using the iterative magic fit function of spdbv. Residues Phe787 and onward of 5J7T were deleted and replaced by residues Phe787 -Gly1078 of 4YOC chain C, which was renamed to chain A. The structure of USP9X (MIM: 300072; pdb entry 5WCH)(41) was then superposed onto the model of USP7; the backbone of pdb entry 5WCH chain A residues Arg1896-Cys1908 and Ala1948-Arg1955 were superposed onto the corresponding residues of the USP7 model (residues Lys476-Cys488 and Ala513-Arg520). Finally, the USP48 sequence (Swiss-Prot entry Q86UV5) was aligned onto the USP7 template.

Human inner ear expression

Human fetal inner ears were collected after elective termination of pregnancy by vacuum aspiration. Fetal age (in weeks, W), defined as the duration since fertilization, was determined by obstetric ultrasonography prior to termination. Tissue was obtained at the following developmental stages: W12 (n = 3), W14 (n = 3), W15 (n= 2), W16 (n = 2), W17 (n = 1). Inner ears were fixed in 4% paraformaldehyde, decalcified and embedded in paraffin as previously described(42). Sections (5 µm) were cut using a HM 355 S rotary microtome (Thermo Fisher Diagnostics). Sections were deparaffinized in xylene and rehydrated, followed by standard immunohistochemistry procedure(42). Sections were incubated overnight at +4°C with a

monoclonal mouse anti-USP48 antibody (1:10, #H00084196-M01, Abnova). Next, sections were incubated with a secondary AF594 donkey anti-mouse antibody (1:500, #A-21203, Thermo Fisher Scientific) for 1h at RT. Nuclei were stained with DAPI. Negative controls were carried out by matching isotype controls and omitting primary antibodies. Positive controls were carried out by conducting isotype control experiments on fetal inner ears (Mouse IgG Isotype Control, #08-6599, Invitrogen). In addition, to compensate for any aspecific binding of secondary antibodies, primary antibodies were omitted. Lastly, positive controls were carried out by staining sections of known positive human tissue samples. Images of these negative controls are presented in Supplementary Figure S3. At least three separate immunostaining experiments for each fetal stage were performed.

Zebrafish model

Zebrafish (Danio rerio, Oregon AB) were maintained at 28.5 °C and on a 14:10 h light/dark cycle and staged by hours (h) or days (d) post fertilization (pf). Eggs were obtained by random mating between sexually mature animals. All procedures complied with both the European Convention for the Protection of Animals used for Experimental and Scientific Purposes and the National Institutes of Health guide for the care and use of Laboratory animals. Housing and experiments were approved by the local authorities, i.e. the Vaud cantonal authority (authorization VD-H21) and INSERM, Montpellier University. We generated founder F0 mutant zebrafish depleted for usp48 by CRISPR/Cas9 genome editing. Three distinct guide (g)RNAs targeting coding sequence in usp48 exon 4 (gusp48-4 5'-AGATGCTCGCAAATCGTCCGTGG-3'), exon 9 (gusp48-9 5'.AGCGCGGTGTTGATTCATCG-3') and exon 10 (gusp48-10 5'.GACAGAAGAGATTAACCAGA-3') were designed using the CHOPCHOP tool(43). The targeted exons are present in the three different usp48 transcripts annotated by Ensembl (Zebrafish GRCz11). Briefly gRNAs were transcribed in vitro using the GenArt gRNA synthesis kit (#A29377, ThermoFisher) according to the manufacturer's instructions. A total of 1 nl of a cocktail containing 100 ng/.l of each gRNA was injected with 200 ng/.l of Cas9 protein (PNA Bio), as treatment, or with the same amount (.l) of water, as control, was injected into one-cell stage embryos. KCl (200 mM) was added to increase the efficiency of the method and Phenol-Red (4x) to visualize the injection. Toxicity of the three guides was compared at 48 hpf while their efficacy was assessed after 72 hpf analyzing fish locomotion. To determine targeting efficiency in founder (F0) mutants, we extracted genomic DNA from 2 dpf embryos and PCR amplified the region flanking the gRNA target site. PCR products were denatured, reannealed slowly and separated on a 20% TBE 1.0-mm precast polyacrylamide gel (Thermo Fisher Scientific), which was then incubated in ethidium bromide and imaged on a ChemiDoc system (Bio-Rad, Hercules, CA) to visualize hetero- and homoduplexes. Targeting efficiency in founder (F0) mutants was also assessed in 5dpf embryos by T7 assay. Briefly, DNA was extracted, and PCR amplified with primers flanking the gRNA target site (5'.CGGACGATTTGCGAGCATCT-3'). PCR products were denatured, reannealed and separated on an agarose gel allowing to assess rearrangements at the targeted site (Supplementary Figure S9).

Locomotion assays

A first qualitative analysis was performed exploiting the touch-response test on 72 hpf larvae, by a slight touch stimulation. The motion of each single larva was examined and scored as « normal swimming », « motionless », « looping swimming » or « pinwheel swimming ». Representative tracking video was obtained with a camera. A second quantitative test was performed analyzing 5 dpf zebrafish spontaneous motility using the Zebrabox® recording system (Viewpoint, Lissieu,

France). Locomotion was recorded for each individual larva on a 96-well plate for 10/15 minutes and presented as slow (3-6 mm/s) and high velocities (>6 mm/s)(44).

Acoustic Startle Response (ASR)

5 dpf zebrafish larvae were transferred to a 96-well plate in 300 µl of water per well and then placed in a ZebraBox® (ViewPoint) inside a soundproof box. After 30 minutes of adaptation, larvae were exposed to three intermittent noise stimulations, 1 second per stimulus. Several frequencies were assessed at 90 dB: 400 Hz, 600 Hz, 800 Hz, 1000 Hz and a broad-band noise, a.k.a. white noise, consisting of all frequencies together. The experiments were performed in light condition. The noise was computer-generated and played through two commercial aerial loudspeakers placed in the chamber. The sound intensity within the box was measured with a noise detector. The variation in ASR were quantified to assess hearing ability. The activity of larvae was automatically and objectively measured before and after sound stimuli and then analyzed. Zebrafish activity was quantified using the quantization mode of ZebraLab® software (Viewpoint)(45). The results were pooled into 1-s time bins to assess ASR.

Visual Motor Response (VMR)

5 dpf zebrafish larvae were transferred to a 96-well plate and then placed inside a ZebraBox® (ViewPoint) equipped with infrared illumination for imaging in the dark itself positioned in a soundproof box. In the box, white light can be controlled accurately. The light-dark protocol consisted of 30 minutes of adaptation in the dark followed by two alternating periods of light (100% of light intensity) and dark of 10 min each one. Zebrafish activity was quantified using the ZebraLab® software (Viewpoint)(45). Data were pooled into 1 min time bins to assess the VMR.

Statistics

Differences between experimental groups were determined by the GraphPad Prism software (version 8.0). Student's t-tests (two-tailed) were performed to analyze behavioral changes in response to noise and light stimulation. The minimum criterion for significance was $p < 0.05$.

Immunohistochemistry of Zebrafish embryos

Zebrafish were treated with 75 .M PTU (1-phenyl 2-thiourea) from 24 hpf to prevent pigmentation. Zebrafish analyzed at 28 hpf were dechorionated before fixation. At appropriate developmental stages, they were anesthetized with 0.0168% tricaine (MS-222, E1052, Sigma-Aldrich) and fixed in 4% PFA for 1 h at RT, permeabilized first in 1X phosphate saline buffer (PBS), 0.5% Triton X-100, for 90 min and subsequently in 1X PBS, 1%Triton X-100, for 2 h on a shaker. Embryos were incubated in blocking buffer (1% BSA in 1X PBS) for 1 h at RT and incubated in primary antibodies overnight at 4°C on a shaker. Primary antibodies were from following sources: mouse anti.synaptotagmin 2 (Znp-1, 1:100, DSHB), mouse anti-islet 1 and 2 (39.4D5, 1:100, DSHB), anti-..bungarotoxin Alexa Fluor™ 555 conjugate (B35451, 1:50, Invitrogen). Following washes with 1X PBS, the embryos were incubated in secondary antibodies overnight at 4°C. For immunofluorescence: Alexa Fluor™ 488 conjugated secondary antibody (1:500) and Phalloidin (1:2000) were used. Nuclei were stained with DAPI (1:8000) for 10 min at RT. Imaging was performed using confocal microscope LSM880 airyscan (Carl Zeiss). Quantification of motor neurons projection lengths was obtained with ImageJ software.

Otoliths, Hair Cells and Statoacoustic neuron structures in Zebrafish Larvae

Zebrafish larvae were analyzed at different timepoints to compare the phenotype and the morphology of specialized structures among treated, controls and wild-type fish. Eggs were obtained by random mating between sexually mature animals (AB line). Some were fixed with

PFA 4% in 1X PBS to assess the distance and dimension of otoliths at 5 dpf, and the morphological phenotype during development from 1 to 5 dpf. Eggs imaging was performed using an optical microscope. Fish length was measured from the head side of the swim bladder to the end of the tail from 3 dpf onwards. Fish length corresponded to the entire animal length from head to tail at 1 and 2 dpf. Other eggs were anesthetized with 0.0168% tricaine (MS-222, E1052, Sigma-Aldrich), bathed in 2 µM of YO-PRO.1 for 30 min, followed by three washes with 1X PBS, to assess the functionality of the hair cells at 3 and 5 dpf. Imaging was performed using a fluorescent macroscope (Olympus). A third group of eggs obtained by mating Brn3c:mGFP females in which hair cells of the inner ear and the lateral line neuromasts are specifically labelled in green(46) and NBT-dsRED males in which the neuronal system is labelled in red (neural-specific beta tubulin promoter driving expression of dsRed red fluorescent protein(47) were anesthetized with 0.0168% tricaine and analyzed at 3, 4 and 5 dpf to assess the structure of the hair cells and statoacoustic neurons expressed in the ear. Imaging was performed using confocal microscope LSM880 airyscan (Carl Zeiss).

Acknowledgments
We thank the affected individuals and their families for their participation in this study. We are grateful to Jacques S. Beckmann for comments. We are indebted to the zebrafish facility and the cell imaging facility of the University of Lausanne and the Montpellier ZebraSens behavioral phenotyping platform (MMDN) in particular to N. Cubedo and J. Sarniguet for help. The Dutch DOOFNL Consortium consisting of M.F. van Dooren, S.G. Kant, H.H.W. de Gier, E.H. Hoefsloot, M.P. van der Schroeff , L.J.C. Rotteveel, F.G. Ropers, J.C.C. Widdershoven, J.R. Hof, E.K. Vanhoutte, I. Feenstra, H. Kremer, C.P. Lanting, R.J.E. Pennings, H.G. Yntema, R.H. Free and J.S. Klein Wassink-Ruiter, R.J. Stokroos, A.L. Smit, M.J. van den Boogaard, F.A. Ebbens, S.M. Maas, A. Plomp, T.P.M. Goderie, P. Merkus and J. van de Kamp, contributed to the clinical evaluation and medical genetic testing of a cohort of ~800 genetically unsolved index cases with hearing loss, evaluated for USP48 variants. SB is recipient of scholarships from the European Social Fund, University of Trieste, Italy and the Fund for Research and Education in Genetics, University of Lausanne, Switzerland. This work was supported by grants from the Swiss National Science Foundation (31003A_182632 to AR and 320030_170062 to FA) and Horizon2020 Twinning project ePerMed (692145) to AR and from the Heinsius-Houbolt foundation to HK. The funders had no role in study design, data collection and analysis, decision to publish, or preparation of the manuscript.

Author contribution
GG and AR conceived and directed the study. SB, AM, NC, MC, FF, RM, SP, JJS, JMvdK, AZ, SM, HK, PG, GG and AR recruited patients, gathered clinical information, prepared samples, performed whole-exome and mutational analysis. SB, MR, NV, YA, BD, FA and TM engineered and phenotyped the zebrafish model. EvB and HL performed the immunohistochemistry. SB, JC and GG carried out the other experiments. NG performed structural modeling of variants. SB performed statistical analysis and analyzed the data. SB and AR wrote the manuscript. All authors reviewed and approved the manuscript.

Conflict of interest
The authors declare no conflict of interest.

Web Resources

ChopChop design tool: http://chopchop.cbu.uib.no gEAR portal: https://umgear.org/#1 Genome Browser: https://genome.ucsc.edu/ GnomAD: https://gnomad.broadinstitute.org/ MaxEntScan: http://hollywood.mit.edu/burgelab/maxent/Xmaxentscan_scoreseq.html NNSplice: https://www.fruitfly.org/seq_tools/splice.html OMIM (Online Mendelian Inheritance in Man): http://www.omim.org The Human Protein ATLAS: https://www.proteinatlas.org/ WHO Deafness and hearing loss: https://www.who.int/health-topics/hearing-loss#tab=tab_1

References

1 Kremer, H. (2019) Hereditary hearing loss; about the known and the unknown. Hear Res, 376, 58-68.

2 Azaiez, H., Booth, K.T., Ephraim, S.S., Crone, B., Black-Ziegelbein, E.A., Marini, R.J., Shearer, A.E., Sloan-Heggen, C.M., Kolbe, D., Casavant, T. et al. (2018) Genomic Landscape and Mutational Signatures of Deafness-Associated Genes. Am J Hum Genet, 103, 484-497.

3 Morgan, A., Koboldt, D.C., Barrie, E.S., Crist, E.R., Garcia Garcia, G., Mezzavilla, M., Faletra, F., Mihalic Mosher, T., Wilson, R.K., Blanchet, C. et al. (2019) Mutations in PLS1, encoding fimbrin, cause autosomal dominant nonsyndromic hearing loss. Hum Mutat, 40, 2286-2295.

4 Eaton, R.C. and Didomenico, R. (1986) Role of the Teleost Escape Response during Development. Transactions of the American Fisheries Society, 115, 128-142.

5 Zeddies, D.G. and Fay, R.R. (2005) Development of the acoustically evoked behavioral response in zebrafish to pure tones. J Exp Biol, 208, 1363-1372.

6 Bruce B. Riley, S.J.M. (2000) Development of Utricular Otoliths, but not SaccularOtoliths, Is Necessary for Vestibular Function andSurvival in Zebrafish. Journal of Neurobiology, 43, 329–337.

7 Busch-Nentwich, E., Sollner, C., Roehl, H. and Nicolson, T. (2004) The deafness gene dfna5 is crucial for ugdh expression and HA production in the developing ear in zebrafish. Development, 131, 943-951.

8 Kazmierczak, M., Harris, S.L., Kazmierczak, P., Shah, P., Starovoytov, V., Ohlemiller, K.K. and Schwander, M. (2015) Progressive Hearing Loss in Mice Carrying a Mutation in Usp53. J Neurosci, 35, 15582-15598.

9 Yokoyama, J.S., Lam, E.T., Ruhe, A.L., Erdman, C.A., Robertson, K.R., Webb, A.A., Williams, D.C., Chang, M.L., Hytonen, M.K., Lohi, H. et al. (2012) Variation in genes related to cochlear biology is strongly associated with adult-onset deafness in border collies. PLoS Genet, 8, e1002898.

10 Akinori SHIMADA, M.E., Takehito MORITA, Takashi TAKEUCHI, Takashi UMEMURA. (1998) Age-Related Changes in the Cochlea and Cochlear Nuclei of Dogs. The Journal of Veterinary Medical Science, 60, 41-48.

11 Ghanem, A., Schweitzer, K. and Naumann, M. (2019) Catalytic domain of deubiquitinylase USP48 directs interaction with Rel homology domain of nuclear factor kappaB transcription factor RelA. Mol Biol Rep, 46, 1369-1375.

12 Lang, H., Schulte, B.A., Zhou, D., Smythe, N., Spicer, S.S. and Schmiedt, R.A. (2006) Nuclear factor kappaB deficiency is associated with auditory nerve degeneration and increased noise-induced hearing loss. J Neurosci, 26, 3541-3550.

13 Kaplanis, J., Samocha, K.E., Wiel, L., Zhang, Z., Arvai, K.J., Eberhardt, R.Y., Gallone, G., Lelieveld, S.H., Martin, H.C., McRae, J.F. et al. (2020) Evidence for 28 genetic disorders discovered by combining healthcare and research data. Nature, 586, 757-762.

14 Monica Fedele, G.M.P., Alfredo Fusco. (2011) The Genetics of Pituitary Adenomas.pdf. Contemporary Aspects of Endocrinology, in press.

15 Chen, J., Jian, X., Deng, S., Ma, Z., Shou, X., Shen, Y., Zhang, Q., Song, Z., Li, Z., Peng, H. et al. (2018) Identification of recurrent USP48 and BRAF mutations in Cushing's disease. Nat Commun, 9, 3171.

16 Uddin, M., Tammimies, K., Pellecchia, G., Alipanahi, B., Hu, P., Wang, Z., Pinto, D., Lau, L., Nalpathamkalam, T., Marshall, C.R. et al. (2014) Brain-expressed exons under purifying selection are enriched for de novo mutations in autism spectrum disorder. Nat Genet, 46, 742-747.

17 Elliott, P.R., Liu, H., Pastok, M.W., Grossmann, G.J., Rigden, D.J., Clague, M.J., Urbe, S. and Barsukov, I.L. (2011) Structural variability of the ubiquitin specific protease DUSP-UBL double domains. FEBS Lett, 585, 3385-3390.

18 Clerici, M., Luna-Vargas, M.P., Faesen, A.C. and Sixma, T.K. (2014) The DUSP-Ubl domain of USP4 enhances its catalytic efficiency by promoting ubiquitin exchange. Nat Commun, 5, 5399.
19 Zimmermann, L., Stephens, A., Nam, S.Z., Rau, D., Kubler, J., Lozajic, M., Gabler, F., Soding, J., Lupas, A.N. and Alva, V. (2018) A Completely Reimplemented MPI Bioinformatics Toolkit with a New HHpred Server at its Core. J Mol Biol, 430, 2237-2243.
20 Blom, N., Sicheritz-Ponten, T., Gupta, R., Gammeltoft, S. and Brunak, S. (2004) Prediction of post-translational glycosylation and phosphorylation of proteins from the amino acid sequence. Proteomics, 4, 1633-1649.
21 Ryals, M., Pak, K., Jalota, R., Kurabi, A. and Ryan, A.F. (2017) A kinase inhibitor library screen identifies novel enzymes involved in ototoxic damage to the murine organ of Corti. PLoS One, 12, e0186001.
22 Dayaratne, M.W., Vlajkovic, S.M., Lipski, J. and Thorne, P.R. (2014) Kolliker's organ and the development of spontaneous activity in the auditory system: implications for hearing dysfunction. Biomed Res Int, 2014, 367939.
23 Vona, B., Doll, J., Hofrichter, M.A.H., Haaf, T. and Varshney, G.K. (2020) Small fish, big prospects: using zebrafish to unravel the mechanisms of hereditary hearing loss. Hear Res, 397, 107906.
24 Kindt, K.S. and Sheets, L. (2018) Transmission Disrupted: Modeling Auditory Synaptopathy in Zebrafish. Front Cell Dev Biol, 6, 114.
25 Cetkovska, K., Sustova, H. and Uldrijan, S. (2017) Ubiquitin-specific peptidase 48 regulates Mdm2 protein levels independent of its deubiquitinase activity. Sci Rep, 7, 43180.
26 Uckelmann, M., Densham, R.M., Baas, R., Winterwerp, H.H.K., Fish, A., Sixma, T.K. and Morris, J.R. (2018) USP48 restrains resection by site-specific cleavage of the BRCA1 ubiquitin mark from H2A. Nat Commun, 9, 229.
27 Truty, R., Paul, J., Kennemer, M., Lincoln, S.E., Olivares, E., Nussbaum, R.L. and Aradhya, S. (2019) Prevalence and properties of intragenic copy-number variation in Mendelian disease genes. Genet Med, 21, 114-123.
28 Velimezi, G., Robinson-Garcia, L., Munoz-Martinez, F., Wiegant, W.W., Ferreira da Silva, J., Owusu, M., Moder, M., Wiedner, M., Rosenthal, S.B., Fisch, K.M. et al. (2018) Map of synthetic rescue interactions for the Fanconi anemia DNA repair pathway identifies USP48. Nat Commun, 9, 2280.
29 Wang, B., Hu, B. and Yang, S. (2015) Cell junction proteins within the cochlea: A review of recent research. J Otol, 10, 131-135.
30 Collado, M.S., Thiede, B.R., Baker, W., Askew, C., Igbani, L.M. and Corwin, J.T. (2011) The postnatal accumulation of junctional E-cadherin is inversely correlated with the capacity for supporting cells to convert directly into sensory hair cells in mammalian balance organs. J Neurosci, 31, 11855-11866.
31 Wang, H.C. and Bergles, D.E. (2015) Spontaneous activity in the developing auditory system. Cell Tissue Res, 361, 65-75.
32 Yamasoba, T., Lin, F.R., Someya, S., Kashio, A., Sakamoto, T. and Kondo, K. (2013) Current concepts in age-related hearing loss: epidemiology and mechanistic pathways. Hear Res, 303, 30-38.
33 Koffler, T., Ushakov, K. and Avraham, K.B. (2015) Genetics of Hearing Loss: Syndromic. Otolaryngol Clin North Am, 48, 1041-1061.
34 Vozzi, D., Morgan, A., Vuckovic, D., D'Eustacchio, A., Abdulhadi, K., Rubinato, E., Badii, R., Gasparini, P. and Girotto, G. (2014) Hereditary hearing loss: a 96 gene targeted sequencing protocol reveals novel alleles in a series of Italian and Qatari patients. Gene, 542, 209-216.
35 Gueneau, L., Fish, R.J., Shamseldin, H.E., Voisin, N., Tran Mau-Them, F., Preiksaitiene, E., Monroe, G.R., Lai, A., Putoux, A., Allias, F. et al. (2018) KIAA1109 Variants Are Associated with a Severe Disorder of Brain Development and Arthrogryposis. Am J Hum Genet, 102, 116-132.
36 Smits, J.J., Oostrik, J., Beynon, A.J., Kant, S.G., de Koning Gans, P.A.M., Rotteveel, L.J.C., Klein Wassink-Ruiter, J.S., Free, R.H., Maas, S.M., van de Kamp, J. et al. (2019) De novo and inherited loss-of-function variants of ATP2B2 are associated with rapidly progressive hearing impairment. Hum Genet, 138, 61-72.
37 Tzimas, C., Michailidou, G., Arsenakis, M., Kieff, E., Mosialos, G. and Hatzivassiliou, E.G. (2006) Human ubiquitin specific protease 31 is a deubiquitinating enzyme implicated in activation of nuclear factor-kappaB. Cell Signal, 18, 83-92.
38 Nicolas Guex, M.C.P. (1997) <SWISS-MODEL and the Swiss-PdbViewer- An environment for comparative protein modeling>. Electrophoresis, 15, 2714-2723.
39 Rouge, L., Bainbridge, T.W., Kwok, M., Tong, R., Di Lello, P., Wertz, I.E., Maurer, T., Ernst, J.A. and Murray, J. (2016) Molecular Understanding of USP7 Substrate Recognition and C-Terminal Activation. Structure, 24, 1335-1345.
40 Cheng, J., Yang, H., Fang, J., Ma, L., Gong, R., Wang, P., Li, Z. and Xu, Y. (2015) Molecular mechanism for USP7-mediated DNMT1 stabilization by acetylation. Nat Commun, 6, 7023.

41 Paudel, P., Zhang, Q., Leung, C., Greenberg, H.C., Guo, Y., Chern, Y.H., Dong, A., Li, Y., Vedadi, M., Zhuang, Z. et al. (2019) Crystal structure and activity-based labeling reveal the mechanisms for linkage-specific substrate recognition by deubiquitinase USP9X. Proc Natl Acad Sci U S A, 116, 7288-7297.
42 Heiko Locher, J.H.F., Liesbeth van Iperen, John CMJ de Groot, Margriet A Huisman & Susana M Chuva de Sousa Lopes (2013) <Neurosensory development and cell fate determination in the human cochlea>. Neural Development, 8.
43 Labun, K., Montague, T.G., Gagnon, J.A., Thyme, S.B. and Valen, E. (2016) CHOPCHOP v2: a web tool for the next generation of CRISPR genome engineering. Nucleic Acids Res, 44, W272.276.
44 Arribat, Y., Mysiak, K.S., Lescouzeres, L., Boizot, A., Ruiz, M., Rossel, M. and Bomont, P. (2019) Sonic Hedgehog repression underlies gigaxonin mutation-induced motor deficits in giant axonal neuropathy. J Clin Invest, 129, 5312-5326.
45 Liu, X., Lin, J., Zhang, Y., Guo, N. and Li, Q. (2018) Sound shock response in larval zebrafish: A convenient and high-throughput assessment of auditory function. Neurotoxicol Teratol, 66, 1-7.
46 Di Donato, V., Auer, T.O., Duroure, K. and Del Bene, F. (2013) Characterization of the calcium binding protein family in zebrafish. PLoS One, 8, e53299.
47 Peri, F. and Nusslein-Volhard, C. (2008) Live imaging of neuronal degradation by microglia reveals a role for v0-ATPase a1 in phagosomal fusion in vivo. Cell, 133, 916-927.

Figures Caption:

Figure 1. Pedigrees and Sanger sequencing.

(A) Pedigree of the Italian family carrying the (c.1216G/A) variant in USP48 (top). Pedigrees of the Dutch presenting the variant (c.2215_2216delinsTT) and French family carrying the variant (c.3058+2T>C) in USP48 (bottom left and right, respectively). Filled symbols represent affected individuals. (B) Sanger sequencing traces confirming the segregation of variant (c.1216G/A) in the Italian family.

Figure 2. 3D modeling and in vitro functional analysis.

(A) USP48 tridimensional protein modeling based on the paralogous USP7 template (blue ribbon). In the model are highlighted the Ubiquitin molecule (yellow), Gly406 mutated in the Italian family (red space-filled residue) within the unstructured loop of residues Tyr498-Asn512 (red ribbon), the equivalent USP9X region bearing residues Phe1921-Asn1947, which form an antiparallel beta-sheet (white ribbon), Met415 mutated in Cushing's disease (green space-filled), three USP48 residues Cys98, His353, Asn370 of the catalytic triad corresponding to USP7 residues Cys223, His464 and Asp481 (orange space-filled). (B) USP48 tridimensional protein modeling of the DUSP domain (salmon ribbon) highlighting the solvent exposed position of Thr739 (red space-filled) that is mutated in Dutch proband. (C) Whereas intolerance to truncating variants is customarily used to narrow down lists of causative variants in autosomal dominant intellectual disability and syndromic developmental disease we assessed if this was a good selection criterion when searching for genes associated with ADNSHHL. To evaluate this criterion, we assessed the distribution of observed over expected (o/e) LoF variants in GnomAD v2.1.1 (n=46 genes, bin width=0.1). The density distribution and the data normalization have been performed through the Kernel density estimation function (KDE). While some ADNSHHL genes are not constrained especially the prevalent ones (e.g., GJB2 o/e = 2.62 and GJB6 o/e = 1.07), we observed that 30 out of 46 ADNSHHL genes (65%) present with an o/e LoF ratio below 0.5. This result suggests that the majority of dominant non-syndromic deafness genes are under evolutionary pressure (o/e median = 0.37) and that this can be used as a selection criterion upon screening for novel rare ADNSHHL causative genes. The o/e ratio of USP48 is indicated with a red line. (D) Ability of the

USP48 alleles to hydrolyze tetra-ubiquitin molecules in tri-, di- and mono-ubiquitin molecules. Ubiquitin multimers are separated by SDS-PAGE after incubation with the USP48 enzyme (FLAG.USP48 Wt, FLAG-USP48G98S catalytically dead, FLAG-USP48G406R, FLAG-USP48T739L and FLAG.USP481-1019) mentioned on top of each lane. Please note that whereas FLAG-USP48 Wt is capable of hydrolyzing tetra-ubiquitin (48kD band), the multiple variants identified in the patients and the catalytically dead variant are impaired. While some intermediate polyubiquitin bands are nevertheless visible in the corresponding lanes it is not possible to distinguish if these results are due to passive degradation of tetra-ubiquitin or residual enzymatic activity of the variants.

Figure 3. USP48 expression in the human fetal inner ear.

Human embryonic ear immunostaining showing DNA (DAPI) in blue and the USP48 protein in green. USP48 is expressed in several structures: (A) at W14, in Kolliker's Organ (KO), the Outer Sulcus (OS), the fibrocytes of the Spiral Ligament (SL), the interdental cells of the spiral limbus (IC), the intermediate cells of the Stria Vascularis (SV) and in Reissner's Membrane (RM), but not in the Inner Hair Cells (IHC) or Outer Hair Cells (OHC); (B) at W14, in the neurons and supporting mesenchyme of the Spiral Ganglion (SG); (C) at W15 in the Periotic Mesenchyme (PM) and the Supporting Cells (SC) of the saccule macula of the vestibular system (pinpointed by asterisks).

Figure 4. usp48 knocked-down zebrafish model.

(A) Touch Test Response of 3 dpf wild-type (Wt; n=71), usp48 knocked-down (gusp48-4+Cas9; treated:T; n=41) and control zebrafish (gusp48-4; mock:M; n=32). (B) Acoustic Startle Response of 5 dpf wild-type (Wt; n>40), usp48 knocked-down (gusp48-4+Cas9; treated:T; n>40) and controls zebrafish (gusp48-4; mock:M; n>40) towards white noise (broad-band noise), 400 Hz, 600 Hz, 800 Hz and 1000 Hz lengths. (C) Maximum projections of confocal images regarding specific neuronal structures in 5 dpf Wt, T and M fish: the statoacoustic neurons (red arrows), Xth ganglia (white arrows) and the posterior lateral line ganglia (PLLG, green ellipses) are indicated in the top panels; the statoacoustic neurons and PPLG are pinpointed with white and green ellipses, respectively, in the bottom panels. (D) Number of statoacoustic neurons (single cell count) in 5 dfp Wt (n=2), T (n=5) and M (n=3) fish. P-value legend: * ≤ 0.02.

Abbreviations

HHL = Hereditary Hearing Loss NSHHL = Non-Syndromic Hereditary Hearing Loss ADNSHHL = Autosomal Dominant Non-Syndromic Hereditary Hearing Loss MAF = minor allele frequency
IHCs = inner hair cells WHO = World Health Organization
ASR = Acoustic Startle Response VMR = Visual Motor Response

Figure 1

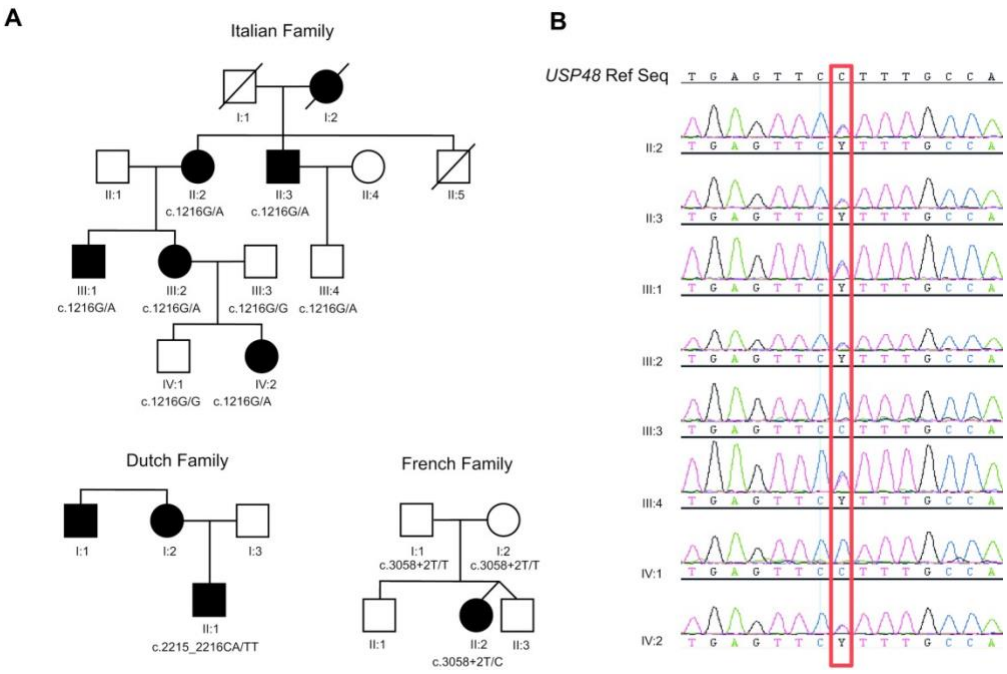
A
Italian Family
I:1
I:2
II:1
II:2
c.1216G/A
II:3
c.1216G/A
II:4
II:5
III:1
c.1216G/A
III:2
c.1216G/A
III:3
c.1216G/G
III:4
c.1216G/A
IV:1
c.1216G/G
IV:2
c.1216G/A
Dutch Family
I:1
I:2
I:3
II:1
c.2215_2216CA/TT
French Family
I:1
c.3058+2T/T
I:2
c.3058+2T/T
II:1
II:2
c.3058+2T/C
II:3
B
USP48 Ref Seq
T G A G T T C C T T T G C C A
II:2
II:3
III:1
III:2
III:3
III:4
IV:1
IV:2

Figure 2

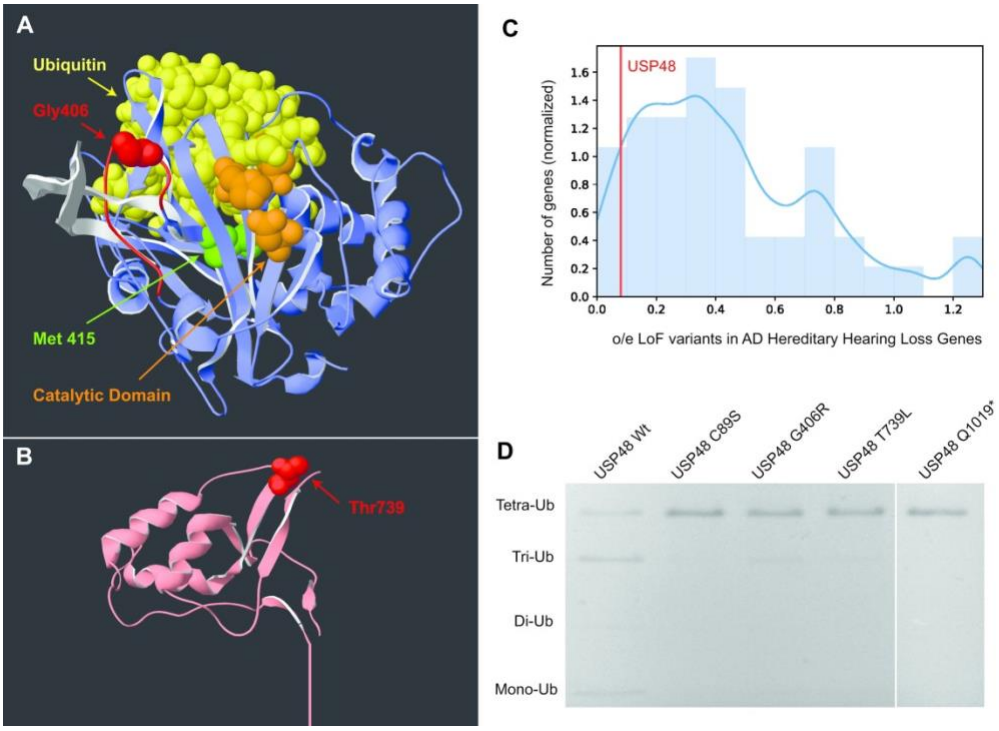
A
Ubiquitin
Gly406
Met 415
Catalytic Domain
B
Thr739
C
USP48
Number of genes (normalized)
o/e LoF variants in AD Hereditary Hearing Loss Genes
D
USP48 WT
USP48 C89S
USP48 G406R
USP48 T739L
USP48 Q1019*
Tetra-Ub
Tri-Ub
Di-Ub
Mono-Ub

Figure 3

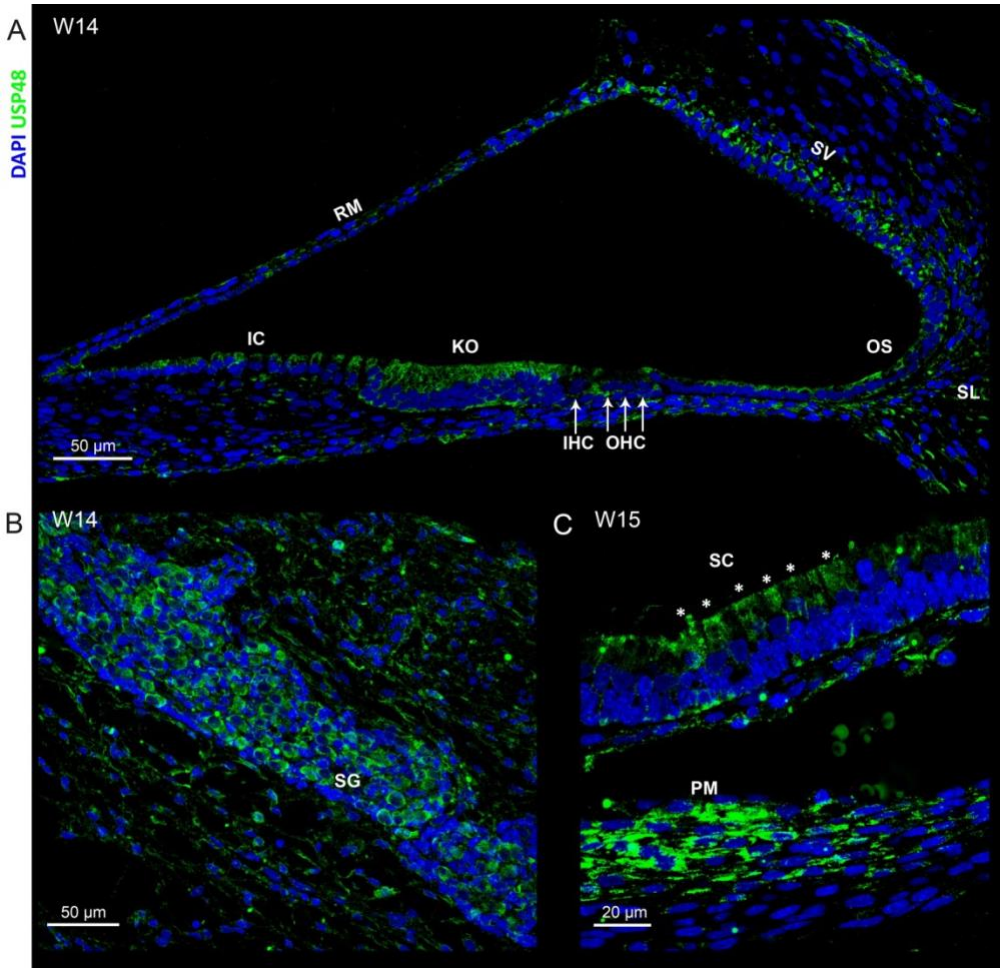
A
W14
DAPI USP48
RM
SV
IC
KO
OS
SL
IHC OHC
50 µm
B
W14
SG
50 µm
C
W15
SC
PM
20 µm

Figure 4

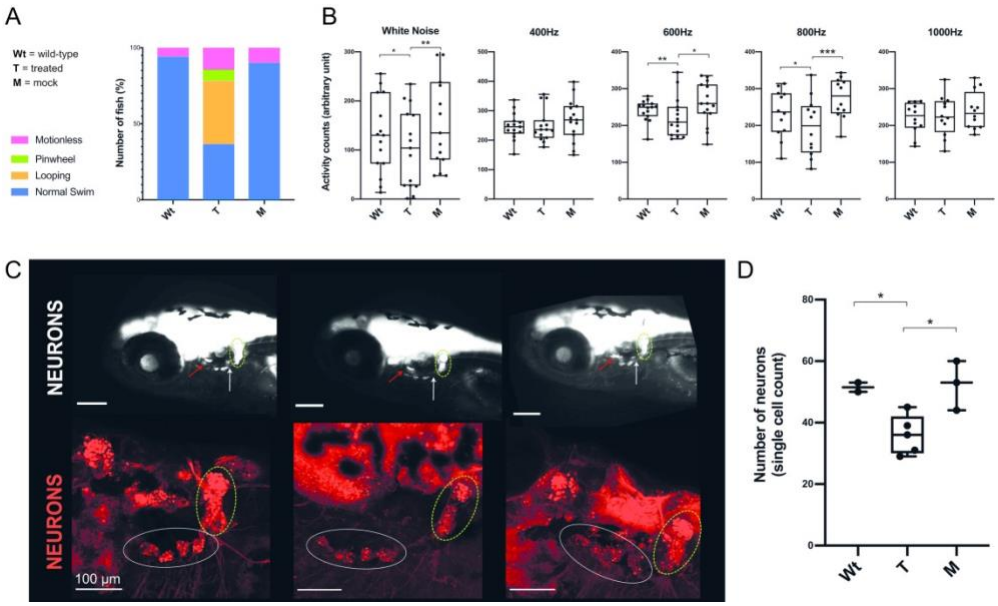
A
Wt = wild-type
T = treated
M = mock
Motionless
Pinwheel
Looping
Normal Swim
Number of fish (%)
Wt
T
M
B
White Noise
400Hz
600Hz
800Hz
1000Hz
Activity counts (arbitrary unit)
C
NEURONS
NEURONS
100 µm
D
Number of neurons (single cell count)

Variants in *USP48* encoding ubiquitin hydrolase are associated with Autosomal Dominant Non-Syndromic Hereditary Hearing Loss

Sissy Bassani *et al*.

Supplementary Materials

Figure S1

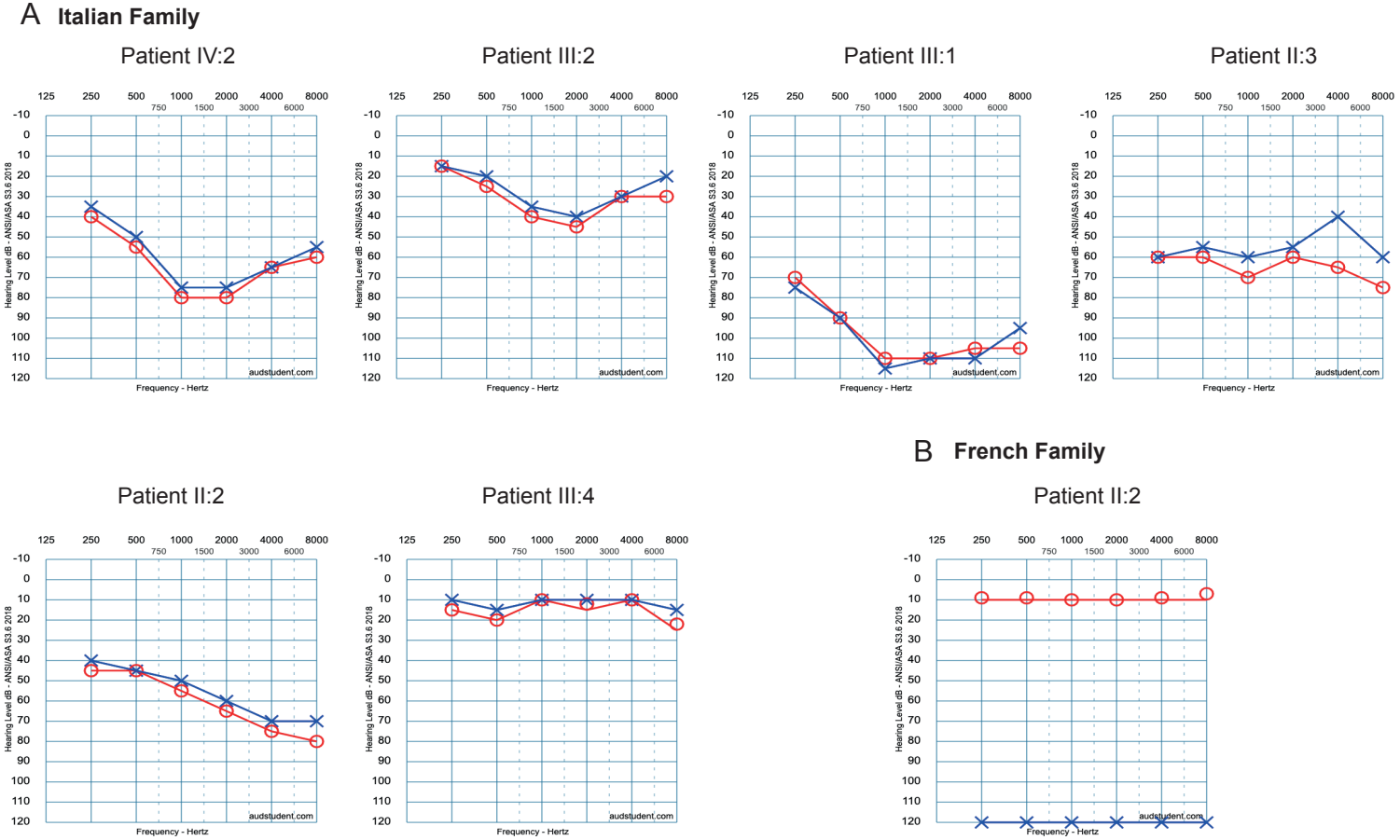

Figure S1. Audiograms.
(A) Audiograms of Italian family members. Patient IV:2: the Italian proband's audiometric test at 21 y.o. shows slight (low frequency) to severe (mid- to high- frequencies) bilateral sensorineural hearing loss. The audiometric test of the proband's mother at 44 y.o (patient III:2) shows moderate (mid-frequencies) to slight (high frequencies) bilateral sensorineural hearing loss. The audiometric test of the proband's maternal uncle at 76 y.o. (patient III:1), presents severe (low frequencies) to profound (mid- to high- frequencies) bilateral sensorineural hearing loss. The proband's grandmother's brother, patient II:3, presents with severe hearing loss across all frequencies at 68 y.o., with the left ear reaching a moderate loss at the 4kHz. Individual III.4, presents normal hearing at all frequencies in both ears at 39 y.o, while the patient II.2 shows moderate (low frequencies) to severe (mid-frequencies) and profound (high frequencies) bilateral sensorineural hearing loss at 72 y.o. **(B)** Audiogram of the French proband (II:2) at 6 y.o. She presents with profound sensorineural hearing loss at all frequencies in her left ear.

Figure S2

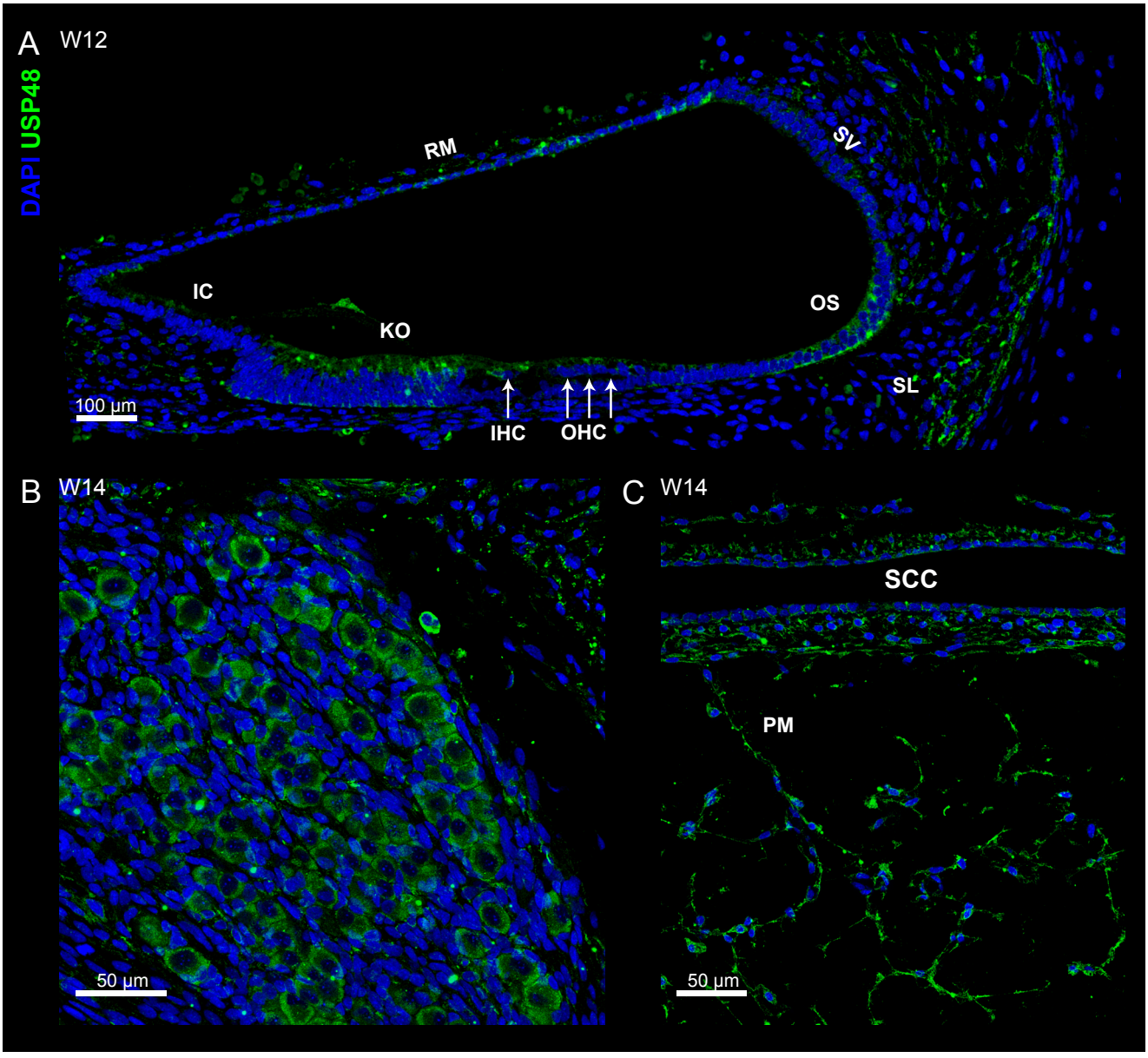

Figure S2. USP48 expression in the human fetal inner ear.
Human embryonic ear immunostaining showing DNA (DAPI) in blue and the USP48 protein in green. USP48 is expressed in several structures: **(A)** at W12, in Kolliker's Organ (KO), the Outer Sulcus (OS), the Spiral Ligament (SL) and in Reissner's Membrane (RM), but not in Inner (IHC) or Outer Hair Cells (OHC), interdental cells (IC) or intermediate cells of the stria vascularis (SV); **(B)** at W14, in neurons of Scarpa's Ganglion; **(C)** at W14, in the epithelial cells of the semicircular canals (SCC) and the periotic mesenchyme (PM) of the vestibular system.

Figure S3

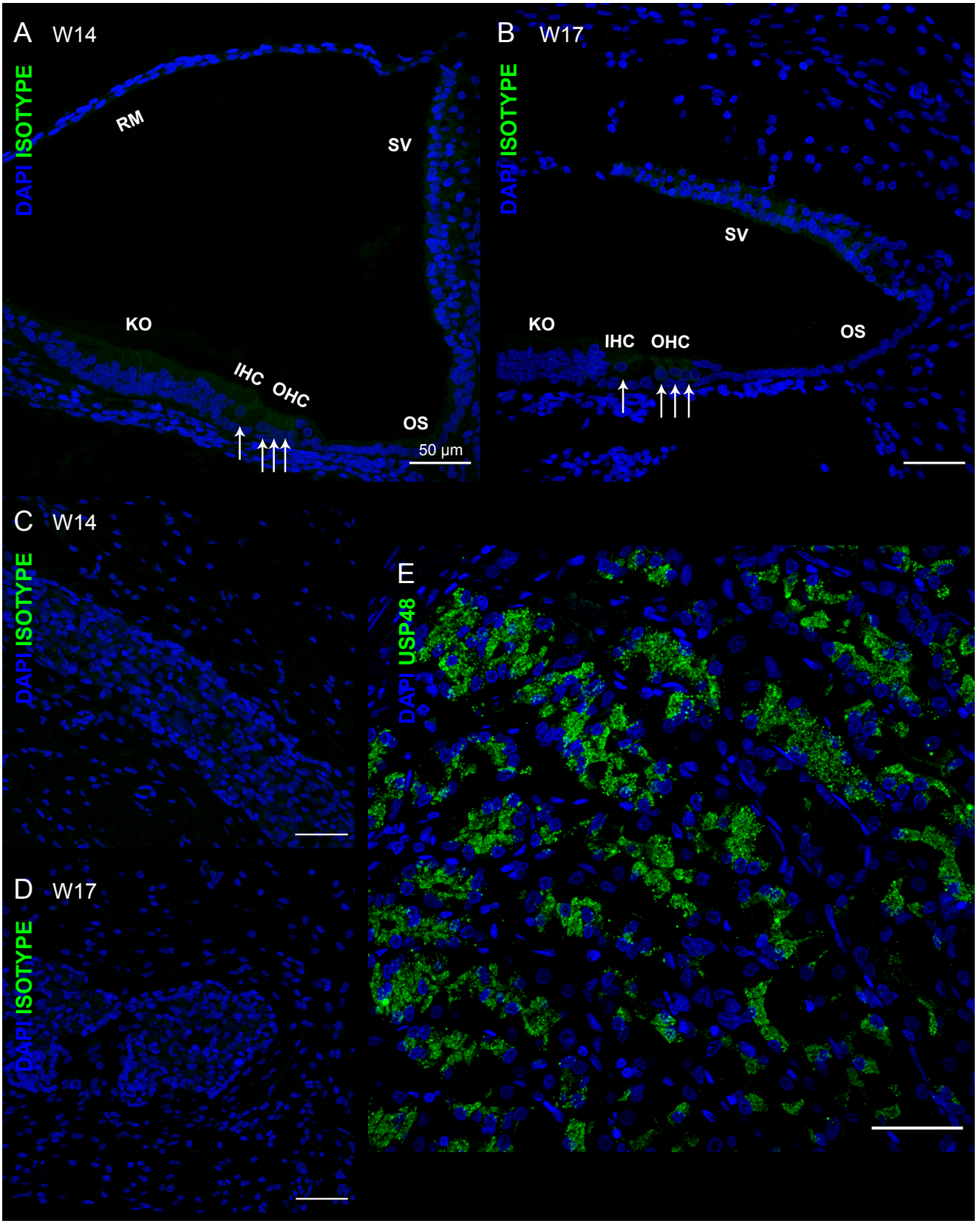

Figure S3. Immunostaining control experiments.
Isotype control experiments were carried out on human fetal inner ears of W14 and W17.
(A,B) Isotype immunostaining of the cochlear basal turn containing Kolliker's Organ (KO), the inner and outer hair cells (IHC, OHC), outer sulcus cells (OS), stria vascularis (SV) and Reissner's membrane (RM), showing absence of aspecific binding. **(C, D)** Immunostaining of the spiral ganglion; no aspecific binding was observed. **(E)** Human oesophagus was used as positive control.

Figure S4

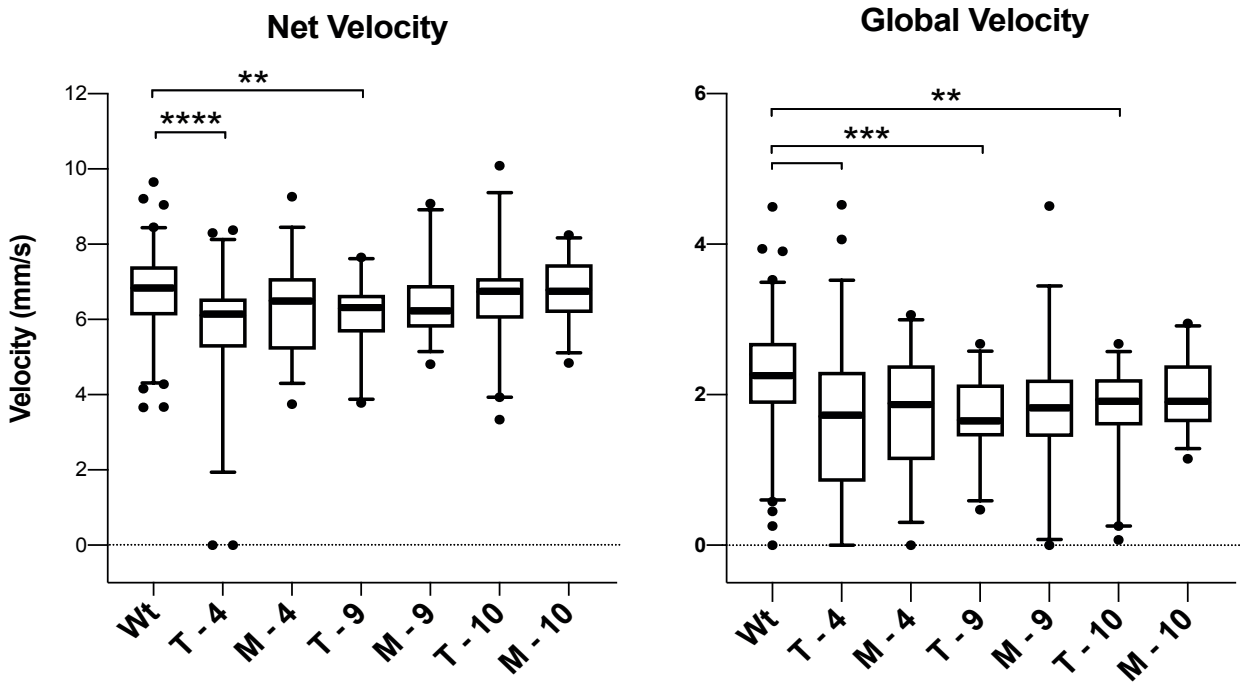

Figure S4. usp48 knocked-down zebrafish model velocity.
Global and net velocity of 5 dpf wild-type (Wt; n=82), usp48 knocked-downs (treated:T) and controls zebrafish (mock-treated:M). Three different guides RNA targeting exon 4, 9 and 10 with (T-4 n=52, T-9 n=33 and T-10 n=39, respectively) or without Cas9 (M-4 n=34, M-9 n=33 and M-10 n=28, respectively) were used. P-value legend net velocity (** = 0.005; **** < 0.0001); global velocity (*** < 0.0006; ** = 0.002).

Figure S5

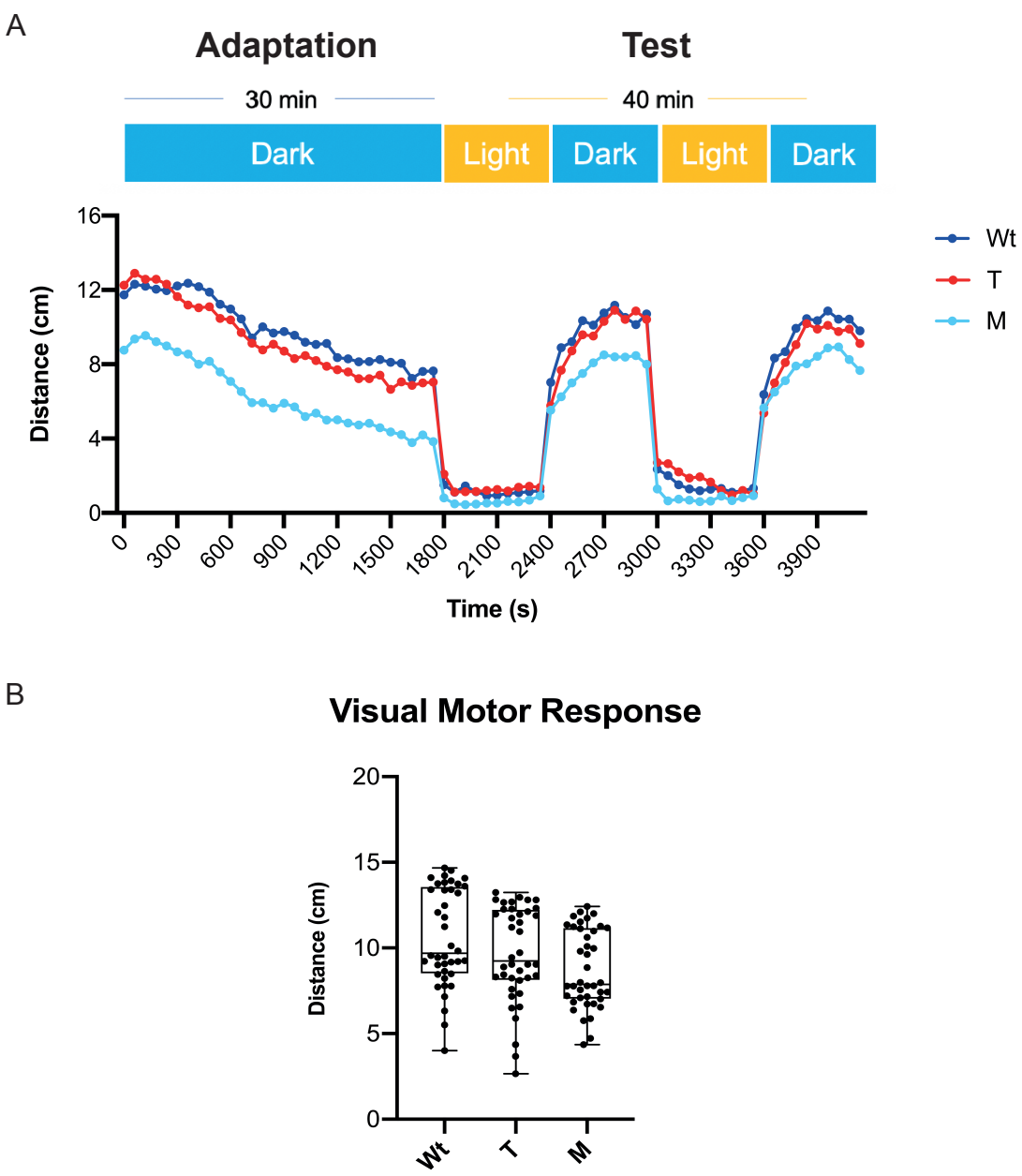

Figure S5. usp48 knocked-down zebrafish model visual motor response (VMR).
The visual ability of 5 dpf wild-type (Wt; n=40), usp48 knocked-down (gusp48-4+Cas9; treated:T; n=40) and controls Zebrafish (gusp48-4; mock:M; n=40) was assessed by measuring the distance travelled during light-dark transitions. **(A)** The light-dark protocol consisted of 30 minutes of adaptation followed by two alternating periods of light and dark every 10 min (600 seconds) as depicted on top. The graph shows the mean distance travelled by fish of the three groups. **(B)** Boxplots of fish reactivity during the two VMR tests considering the mean activity during the dark periods normalized with the mean activity during the light periods.

Figure S6

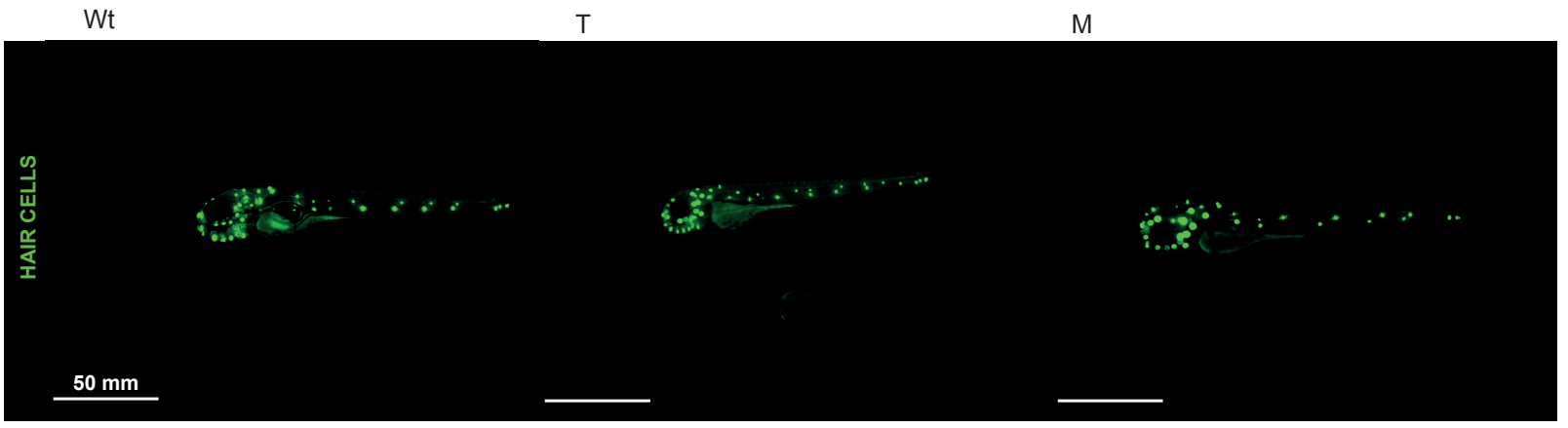

Figure S6. Neuromasts of usp48 knocked-down zebrafish model.
Distribution of neuromasts in wild-type (Wt; n>10), usp48 knocked-down (gusp48-4+Cas9; treated:T; n>10) and controls Zebrafish (gusp48-4; mock:M; n>10) along the anterior (head) and posterior (trunk and tail) lateral-line systems. The YO-PRO-1 drug allowed assessing the receptive activity of hairs of the sensory hair cells.

Figure S7

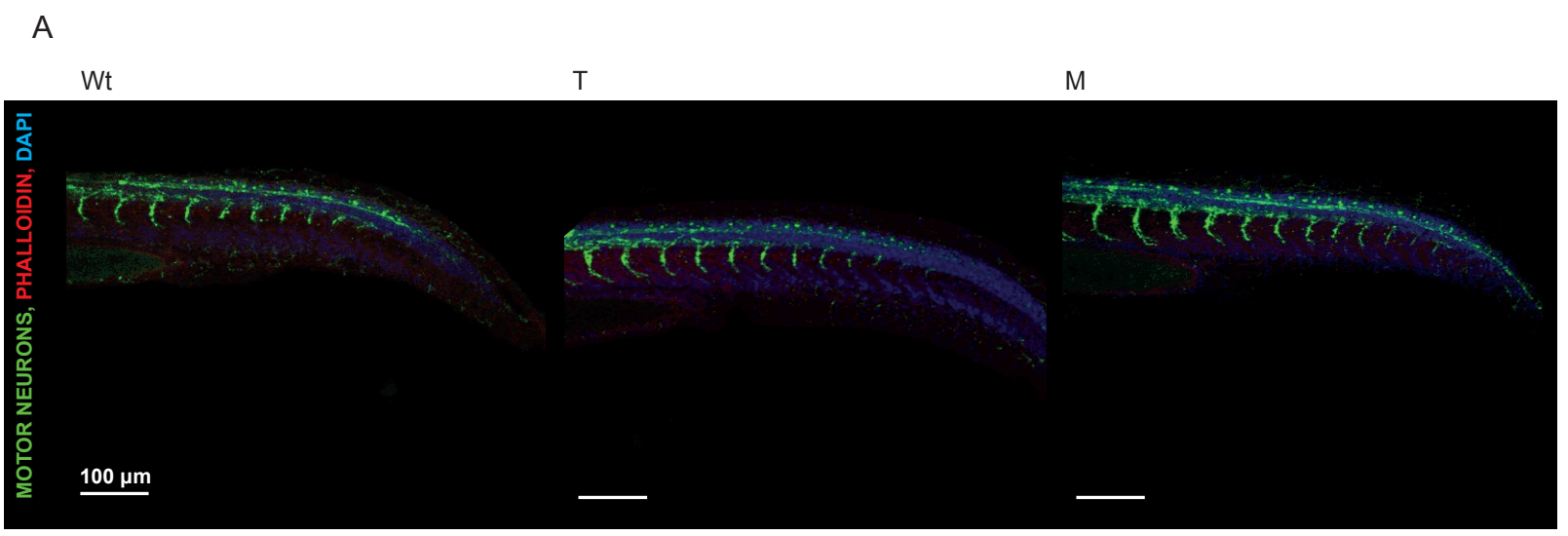

Figure S7. Development of primary motor neurons of usp48 knocked-down zebrafish model.
(A) Primary motor neurons (green), DNA (DAPI-stained, blue) and F-actin (red) of 28 hpf wild-type (Wt), usp48 knocked-down (treated:T) and controls zebrafish (mock:M). **(B)** Boxplots of primary motor neurons length of 28, 48 and 72hpf of wild-type (Wt; 28hpf n=4; 48hpf n=4; 72hpf n=4), usp48 knocked-down (gusp48-4+Cas9; treated:T; 28hpf n=9; 48hpf n=4; 72hpf n=9) and controls zebrafish (gusp48-4; mock:M; 28hpf n=8; 48hpf n=2; 72hpf n=3). P-value legend: * = 0.01; ** = 0.002; **** < 0.0001.

Figure S8

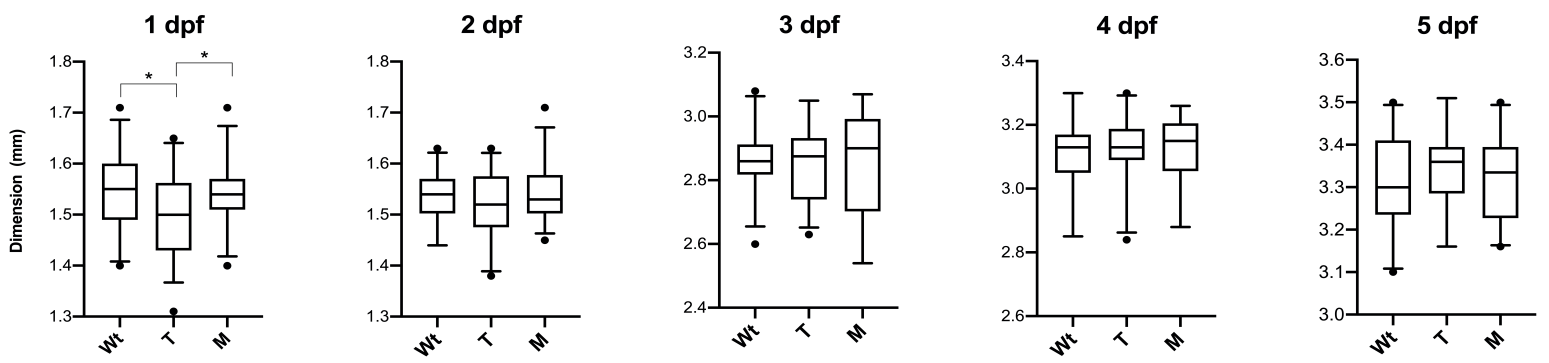

Figure S8. Morphology of usp48 knocked-down zebrafish model.
Fish size during the first five days after fertilization of wild-type (Wt; 1dpf n=27 ; 2dpf n=36; 3dpf n=30; 4dpf n=19; 5dpf n=21), usp48 knocked-down (gusp48-4+Cas9; treated:T; 1dpf n=38 ; 2dpf n=37; 3dpf n=30; 4dpf n=22; 5dpf n=17) and controls zebrafish (gusp48-4; mock:M; 1dpf n=37; 2dpf n=33; 3dpf n=18; 4dpf n=17; 5dpf n=23). P-value legend: * < 0.02.

Figure S9

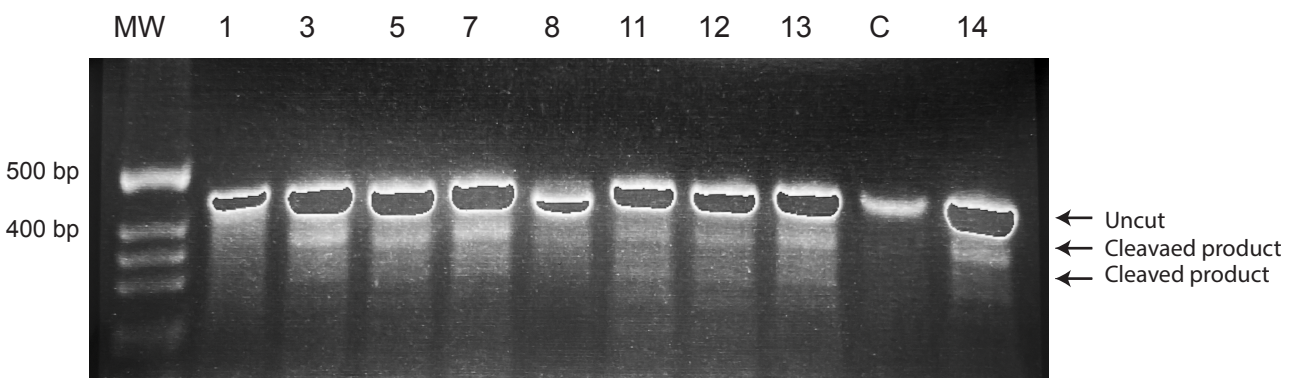

Figure S9. Identification of heteroduplex DNA fragments.
PCR fragments across the CRISPR target region were amplified using Hot Start High-Fidelity Master Mix from DNA of 5dpf treated fish (lanes numbered 1,3,5,7,8,11,12,13,14) and one uninjected control (lane C). Agarose gel electrophoresis of nuclease-treated PCR products to visualize homo- and heteroduplexes, indicative of small indels (cleaved product) is shown.

Table S1. Constraints of genes associated to Autosomal Dominant Non-Syndromic Hereditary Hearing Loss (NSHHL).

Autosomal Dominant HHL gene	OMIM number	pLI[1]	o/e LoF[2]	Z missense[3]	o/e missense[4]
ACTG1	604717	0	0.43	3.16	0.37
CCDC50	607453	0	0.49	0.07	0.99
CD164	616969	0.49	0.19	-0.26	1.07
CEACAM16	614616	0	0.61	0.52	0.91
COCH	601369	0	0.59	0.68	0.89
COL11A1	618533	1	0.14	1.02	0.91
COL11A2	601868	0.7	0.22	2.37	0.79
CRYM	616357	0.03	0.36	0.98	0.79
DFNA5	608798	0	0.74	-0.84	1.15
DIABLO	605219	0	0.77	-1.12	1.28
DIAPH1	602121	0.92	0.2	1.65	0.82
EYA4	601316	0.05	0.27	1.12	0.83
GJB2	121011	0	2.62	-0.72	1.17
GJB3	612644	0	0.63	-0.53	1.11
GJB6	612643	0	1.07	0.45	0.9
GRHL2	608641	1	0.13	1.93	0.71
HOMER2	616707	0.01	0.35	0.31	0.94
IFNLR1	607404	0.06	0.33	0.77	0.87
KCNQ4	600101	0.47	0.22	2.17	0.7
KITLG	616697	0.85	0.13	0.81	0.81
LMX1A	601412	0.99	0.09	1	0.81
MCM2	116945	0	0.38	1.68	0.81
MYH14	600652	0.04	0.24	2.28	0.82
MYH9	603622	1	0.04	3.47	0.71
MYO3A	606808	0	0.86	-0.13	1.01
MYO6	606346	0	0.3	1.39	0.85
MYO7A	601317	0	0.7	1.07	0.92
NLRP3	606416	0	0.33	2.14	0.74
OSBPL2	616340	0.13	0.26	1.97	0.67
P2RX2	608224	0	0.96	0.23	0.96
PDE1C	618140	0	0.49	1.39	0.81
PLS1	618787	0	0.43	1.48	0.77
POU4F3	602459	0.92	0	0.66	1.14
PTPRQ	617663	0	0.55	1	0.91
REST	612431	0.99	0.12	0.78	0.91
SCD5	619086	0	0.49	0.92	0.82
SIX1	605192	0.65	0.17	1.19	0.74
SLC17A8	605583	0	0.36	0.83	0.87
TBC1D24	616044	0	0.73	0.76	0.89
TECTA	601543	0	0.45	1.61	0.87
TECTB	602653	0	0.85	-0.12	1.02
TJP2	613558	0	0.46	0.57	0.94
TMC1	606705	0	0.74	0.86	0.88
TNC	615629	0	0.33	-0.08	1.01
TRRAP	618778	1	0.03	8.17	0.52
WFS1	600965	0	1.62	-4.71	1.55
USP48	617445	1	0.08	4.37	0.47

[1] pLI = probability of being loss-of-function (LoF) intolerant
[2] o/e LoF = ratio of observed / expected (o/e) number of loss-of-function variants
[3] the Z missense score indicate if the transcript is intolerant to variation (more constrained).
[4] o/e missense = ratio of observed / expected (o/e) number of missense variants